



Data driven eco efficiency in MDF manufacturing using lignin based resin and waste utilization: Explainable ML for optimization of global warming potential and primary energy demand

Caner Yetis^{1,*}, Merve Tuna Kayılı²

¹ Bitlis Eren University, Vocational School of Technical Sciences, Bitlis, Türkiye

² Karabük University, Department of Architecture, Karabük, Türkiye

* Corresponding author: C. Yetis (cyetis@beu.edu.tr)

<https://doi.org/10.31462/jcemi.2026.691>

Received 8 March 2026; Revised 3 June 2026; Accepted 8 June 2026; Available online 22 June 2026

Keywords

Medium density fiberboard (MDF)
Life cycle assessment (LCA)
Machine learning
Global warming potential
Primary energy demand

Abstract

Medium density fiberboard (MDF) production creates environmental burdens mainly through resin consumption, energy intensive pressing, and material losses. This study developed a Grey Wolf Optimizer (GWO) enhanced machine learning framework to predict global warming potential (GWP) and primary energy demand (PED) using directly controllable MDF process variables. Resin ratio, waste ratio, press temperature, press pressure, and press time were used as inputs, while GWP and PED were defined as outputs. A dataset of 60 production scenarios was used to train four GWO optimized models: CatBoost, Gradient Boosting Machine, Random Forest, and Extra Trees Regressor. Model performance was evaluated using R, R², RMSE, RMSRE, RRMSE, MAE, and MAPE. GWO CatBoost achieved the best GWP prediction performance with test values of R² = 0.9467, RMSE = 10.81, MAE = 8.31, and MAPE = 1.46%, while GWO GBM provided the highest PED accuracy with R² = 0.9214, RMSE = 173.92, MAE = 153.23, and MAPE = 2.22%. SHapley Additive exPlanations (SHAP) analysis identified resin ratio as the dominant predictor for both outputs, followed by press time and press temperature, while waste ratio and press pressure had smaller but meaningful effects. Individual Conditional Expectation (ICE) results showed that higher resin content and more energy intensive pressing conditions generally increased GWP and PED. Overall, the proposed framework provides a rapid and explainable decision support tool for environmentally informed MDF process optimization.

1. Introduction

Medium density fibreboard (MDF) is an engineered wood panel used in numerous applications within interior components and the construction sector. Consequently, its production-related environmental impacts are becoming increasingly significant in building scale assessments [1]. The growing demand for sustainable building materials is accelerating circularity-focused approaches, such as utilising wood waste in panel production, and placing panels like MDF at the centre of the resource efficiency agenda. New applications where MDF can be used as a functional component in interior spaces require the material to be directly linked to its energy and environmental performance [2]. Pressing conditions and mat properties in MDF production play a decisive role in the structure and quality indicators of the board, necessitating the systematic management of production control variables [3].

In energy intensive steps such as fibre drying, efficiency variations dependent on temperature and duration demonstrate that energy performance in production processes must be considered alongside process parameters [4]. When the entire production cycle is considered, it is evident that the total environmental impact is influenced by holistic process management, as energy consumption is sensitive to process settings. Life cycle assessment quantifies the environmental impacts of a product throughout the processes from raw material procurement for a specific functional unit to its exit from the production facility, providing a robust framework for identifying the primary sources of impact in MDF production [5]. Cradle to gate assessments comparing MDF with similar panel products show that the environmental impact is concentrated particularly in the production of raw materials and auxiliary materials and in the board production stage, with transport having a relatively limited share [6].

Systematic literature reviews on wood based panels emphasise that the results of studies in fundamental categories such as climate change are sensitive to production scenarios and data sets, and therefore methodological consistency is critical [7]. Industrial LCA reports prepared using the sector average approach show that the declaration unit is mostly considered as one cubic metre of finished MDF and that energy and binder usage are clearly reflected in the results [8]. In interpreting the climate impacts of wood and wood based products in the construction sector, it is considered that carbon sequestration and scenario assumptions, in addition to emissions during the production phase, also influence the perception of outcomes [9]. The latest PCR documents published for EPD production in construction products aim to strengthen data consistency with module definitions and reporting expectations, and to increase the comparability of LCA outputs for panel products [10]. The EN 15804 A2 compliant PCR approach contributes to standardisation in areas such as system boundaries, data quality and communication formats for wood and wood-based products, thereby promoting the use of LCA outputs [11].

As a significant portion of the environmental impact in MDF production is associated with the production and use of binding chemicals, the resin composition and ratio are among the fundamental components of sustainable production strategies [12]. Recent reviews on the integration of lignin into adhesives demonstrate that lignin can be incorporated into resin systems due to its functional groups and has the potential to reduce dependence on fossil based components [13]. Research into entirely bio based and formaldehyde free adhesive alternatives has revealed that new binding chemistries represent an important area of research in terms of applicability and environmental performance within the panel industry [14]. Current analyses evaluating the techno-economic and cradle to gate environmental impacts of bio-adhesives together show that the transition to binders must be addressed not only in environmental terms but also in terms of scalability and cost [15]. Evaluations conducted on the industrial-scale production of new lignin based polymers and resins indicate that lignin-derived solutions are positioned as a potential pathway for transitioning to different adhesive technologies [16]. Studies comparing the life cycle impacts of formaldehyde based adhesives reveal that the choice of binder can create significant differences in climate impact and energy indicators [17]. Studies examining the cradle to gate profiles of bio-based adhesives as alternatives to traditional resins indicate that the choice of binder is one of the primary areas of intervention for environmental improvement in panel products [18]. However, LCA applications may struggle to provide rapid decision support based on production parameters due to the increasing computational load as data collection costs and the number of scenarios rise [19].

Comprehensive reviews compiling studies that use LCA and machine learning together show that ML methods are increasingly being used in stages such as inventory

estimation, impact estimation, and interpretation support [20]. A recent review systematically comparing the performance of machine learning algorithms in LCA studies reports that different model families can excel in different data types and that model selection depends on the problem structure [21]. Studies addressing ML based decision support in the context of prospective LCA demonstrate that it is possible to generate forecasts with limited data in early stage technology and process design, and that this accelerates scenario scanning [22]. Recent studies on LCA integration in the early design phase reveal that the need for rapid assessment has become particularly evident in decisions regarding building products and components, increasing the demand for data driven tools [23]. Methods based on estimating LCA labels with limited inputs offer an approach that enables the acceleration of LCA calculations in the early phase and the rapid elimination of alternatives [24]. Studies applying LCA and ML integration in concrete design examples demonstrate that environmental indicators can be estimated with high accuracy using appropriate validation strategies and that the design space can be rapidly scanned [25]. Machine learning-based models enable the exploration of large parameter spaces by providing low latency predictions in systems requiring expensive computation or experimentation, thereby strengthening scenario-based decision support [26]. However, the reliable use of models depends on the explainable reporting of variable contributions and the generation of interpretations consistent with engineering intuition. Recent studies demonstrating explainability approaches such as SHAP through concrete applications reveal that making variable importance and interactions visible increases the transferability of model outputs to decision makers.

Although previous studies have made substantial contributions to the environmental assessment of MDF and wood based panel production, several limitations remain in the current literature. Most existing LCA studies report environmental impacts for fixed production scenarios and identify critical process stages, such as resin consumption, electricity use, and pressing operations. However, these studies generally do not provide a rapid predictive framework that links directly controllable production variables with environmental indicators. Similarly, studies on lignin based adhesives and waste utilization mostly focus on material substitution potential, technical feasibility, or comparative environmental performance. In contrast, the combined effects of resin ratio, waste fibre ratio, and pressing conditions on GWP and PED are rarely evaluated within the same decision space. In addition, although the integration of machine learning methods into LCA studies has increased, their application to MDF production remains limited. This limitation is particularly evident in terms of explainable models that reveal the direction and relative contribution of individual production parameters to environmental impacts.

To address this gap, this study develops interpretable machine learning proxy models that predict, with high

accuracy and in a short time, the global warming potential and primary energy demand indicators for one cubic metre of MDF. Directly controllable production variables, including resin ratio, waste ratio, press temperature, press pressure, and press time, were used as model inputs. The study offers a practical decision support approach that reduces the data collection and computational costs associated with conventional life cycle assessment applications as the number of production scenarios increases. The fundamental contribution of the study is that it does not merely report environmental indicators. It also disaggregates the effects of production control variables using explainability tools and demonstrates with numerical evidence which parameters should be prioritized in environmental improvement strategies. By addressing climate impact and energy demand indicators simultaneously, the study reveals relationships that single metric assessments may overlook and demonstrates that environmental eco efficiency can be managed by jointly adjusting production parameters. Therefore, the current research provides a data driven and actionable framework that links sustainability goals in MDF production to operational decisions. In this context, the originality and significance of the study are embodied in the following elements:

- By utilising process variables that can be directly adjusted in MDF production, GWP and PED indicators for one cubic metre of product can be predicted in a short time.
- Through explainability analysis, the contributions of resin ratio, waste ratio, and pressing conditions to environmental outputs are quantitatively separated, and key improvement levers are prioritized.
- Considering GWP and PED indicators together makes the relationships between climate impact and energy demand visible within the same decision space.

- Evaluating lignin based resin ratio and waste utilization rate together with process parameters enables resource efficiency and low carbon targets to be linked with process management.
- In addition to reporting model performance, the outputs generate insights that can be directly transferred to operational decisions, such as production window selection and parameter prioritization.

2. Research Background

2.1. Medium density fibreboard (MDF) production

Medium density fibreboard (MDF) is a composite panel production process based on separating wood raw material into fibres, combining them with binding resins, and pressing them under high temperature and pressure. The production process generally begins with debarking and chipping logs. The resulting wood chips are separated into fibres in defibrators using steam and mechanical action. At this stage, synthetic resins such as urea formaldehyde and additives such as paraffin are added to the fibres to impart water repellent properties. The resin coated fibres are dried in a drying unit to the appropriate moisture level and then spread to form a homogeneous fibre mat. The fibre layer is compressed in hot presses under specific temperature, pressure and pressing time conditions to form MDF boards. In these production stages, the resin ratio, pressing conditions, and the amount of waste generated during production directly affect both product quality and the energy consumption and environmental impact of the production process. Therefore, the MDF production process is considered a production system where critical parameters are controlled in terms of resource efficiency and environmental performance improvement (Fig. 1).

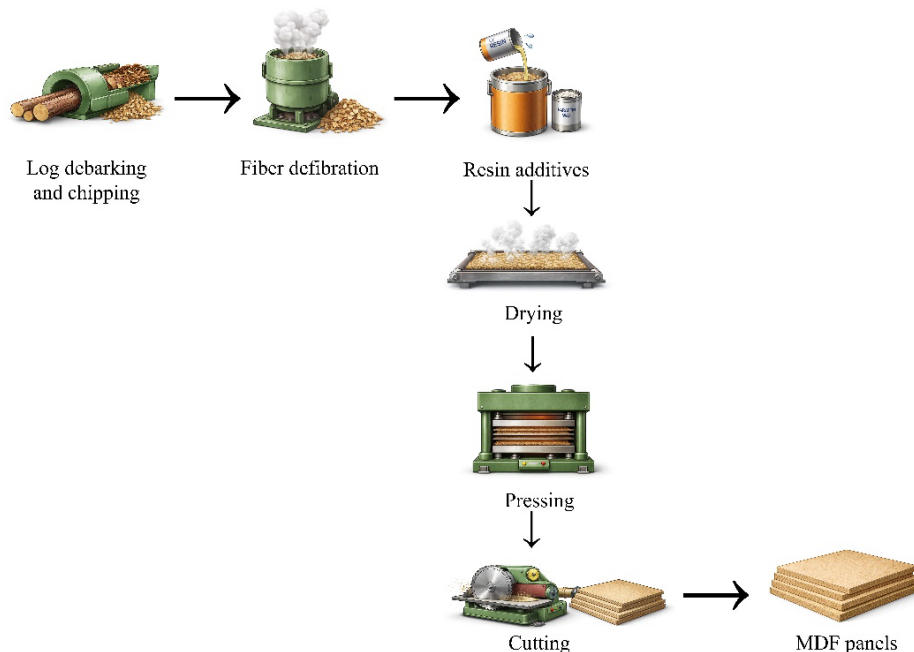


Fig. 1. MDF production process

2.2. Machine learning (ML) algorithms and optimization

2.2.1. Random forest (RF)

Random Forest (RF) is a machine learning method that improves predictive accuracy by combining multiple decision trees. In this approach, numerous training subsets are generated through random sampling of the original dataset. At each node of the trees, splits are performed using randomly selected predictor variables, allowing diverse decision structures to be formed. This mechanism reduces correlation among trees and enhances the generalization capability of the model. During the training process, prediction errors are monitored and utilized to estimate the relative importance of the variables. The mathematical formulation of the final RF prediction is presented in Eq. (1).

$$\hat{y}(x) = \frac{1}{T} \sum_{t=1}^T h_t(x) \quad (1)$$

Here, T represents the total number of trees in the forest, $h_t(x)$ represents the output given by the t -th decision tree to the input, and $\hat{y}(x)$ represents the final prediction of RF. Accordingly, the RF approach is regarded as a machine learning method capable of achieving high predictive performance in the analysis of complex datasets. [27].

2.2.2. Gradient boosting machine (GBM)

Gradient Boosting Machine (GBM) is a machine learning technique in which decision trees sequentially improve the model by correcting the errors of previous trees. The process begins with a simple decision tree, and the model is iteratively updated by learning from the residual errors produced at each stage. In each iteration, the algorithm adjusts the model by focusing on the mistakes made in the previous step, thereby progressively improving predictive performance. The GBM algorithm advances by considering both the direction and magnitude of the error rate, allowing new trees to be added in a way that minimizes these errors. This sequential learning structure enables GBM to capture complex relationships within the data with high accuracy when the model is properly constructed. The formulation of the model at the m th iteration is presented in Eq. (2).

$$F_m(x) = F_{m-1}(x) + v_m h_m(x) \quad (2)$$

Here, $F_m(x)$ m -th iteration model, $F_{(m-1)}(x)$ previous model, $h_m(x)$ m -th added weak learner, and v represents the learning rate [28].

2.2.3. Extra trees regressor (ETR)

Extra Trees Regressor (ETR) is an ensemble learning method that produces predictions by averaging the outputs of multiple decision trees. In this approach, both the selection of variables and the determination of split points are performed randomly during tree construction. This high level of randomness reduces the correlation between individual trees and improves the overall predictive performance of the model. At the same

time, the method helps decrease the risk of overfitting. Owing to this structure, the ETR algorithm provides a flexible modeling framework that is robust to noise and variability in the data. The mathematical representation of the final output produced by the ETR model is presented in Eq. (3).

$$\hat{f}(u) = \frac{1}{K} \sum_{k=1}^K g_k(u) \quad (3)$$

Where; K the total number of trees, $g_k(u)$ the estimate of the k -th extra tree, u represents the input vector [29].

2.2.4. CatBoost

CatBoost (Categorical Boosting) is a gradient boosting algorithm based on decision trees and is being developed as a powerful machine learning method that provides high accuracy. This algorithm is based on the boosting approach, and the model is created by sequentially training decision trees used as weak learners. Each new tree is trained to reduce the prediction errors of the previous model, thereby iteratively improving the model. One of the most important features of the CatBoost algorithm is that it reduces data leakage and limits the overfitting problem by using the ordered boosting approach. The algorithm also incorporates special techniques for processing categorical variables, thereby reducing the need for data pre-processing. Thanks to these features, CatBoost can successfully model non-linear relationships in complex data structures and offers high generalisation performance [30]. The model structure in the CatBoost algorithm is based on binary decision trees. Within this structure, each leaf node is assigned a specific value, and this value represents the predicted target output for the relevant data point. Thus, the model enables the prediction of the target variable through the leaf nodes formed by the decision trees. The mathematical representation of a decision tree is expressed in Eq. (4).

$$h(x) = \sum_{j=1}^J b_j 1_{\{x \in R_j\}} \quad (4)$$

Here, R_j denotes the data regions corresponding to the leaf nodes of the decision tree. Following this stage, statistical values relating to the target variable are calculated for each region (Eq. 5).

$$\hat{x}_k^i = \frac{\sum_{j=1}^n 1_{\{x_j^i = x_k^i\}} y_j + ap}{\sum_{j=1}^n 1_{\{x_j^i = x_k^i\}} + a} \quad (5)$$

Subsequent calculations are performed with the aim of minimising the loss function of the base predictor (Eq. 6).

$$h^t = \arg \min_{h \in H} \frac{1}{n} \sum_{k=1}^n (-g^t(x_k, y_k) - h(x_k))^2 \quad (6)$$

2.2.5. Grey wolf optimizer (GWO)

The Grey Wolf Optimizer (GWO) is a metaheuristic optimization algorithm inspired by the social hierarchy and cooperative hunting behavior of grey wolves. In this algorithm, candidate solutions are categorized into four

hierarchical groups: alpha, beta, delta, and omega. The alpha wolf represents the best solution found so far, while the beta and delta wolves assist in guiding the search process toward promising regions of the solution space. The omega wolves follow the leading groups and contribute to the exploration of new search areas. Key hunting behaviors of grey wolves, such as encircling prey, tracking its movement, and attacking at the appropriate moment, are modeled mathematically within the algorithm. During the optimization process, control parameters are gradually reduced to shift the search from global exploration to local exploitation. Owing to these mechanisms, GWO demonstrates effective performance in solving complex optimization problems [31]. The mathematical formulation describing the prey encircling behavior of grey wolves is presented in Eq. (7).

$$\vec{D} = |\vec{C} \cdot \vec{X}_p(t) - \vec{X}(t)| \vec{X}(t+1) = \vec{X}_p(t) - \vec{A} \cdot \vec{D} \quad (7)$$

Where t repetition, \vec{A} and \vec{C} coefficient vectors, \vec{X}_p the location of the prey, \vec{X} shows the location of the gray wolf. Accordingly, vectors \vec{A} and \vec{C} are calculated using Eq. (8).

$$\vec{A} = 2\vec{a} \cdot \vec{r}_1 - \vec{a} \quad \vec{C} = 2 \cdot \vec{r}_2 \quad (8)$$

Where \vec{a} decreases linearly from 2 to 0 throughout the iterations. \vec{r}_1 and \vec{r}_2 are vectors randomly selected from the interval [0,1]. At this stage, the best three solutions are recorded, and the best search position update is performed. The mathematical equations related to the update are presented in Eqs. (9, 10 and 11).

$$\vec{D}_\alpha = |\vec{C}_1 \cdot \vec{X}_\alpha - \vec{X}|, \vec{D}_\beta = |\vec{C}_2 \cdot \vec{X}_\beta - \vec{X}|, \vec{D}_\delta = |\vec{C}_3 \cdot \vec{X}_\delta - \vec{X}| \quad (9)$$

$$\vec{X}_1 = \vec{X}_\alpha - \vec{A}_1 \cdot (\vec{D}_\alpha), \vec{X}_2 = \vec{X}_\beta - \vec{A}_2 \cdot (\vec{D}_\beta), \vec{X}_3 = \vec{X}_\delta - \vec{A}_3 \cdot (\vec{D}_\delta) \quad (10)$$

$$\vec{X}(t+1) = \frac{\vec{X}_1 + \vec{X}_2 + \vec{X}_3}{3} \quad (11)$$

3. Methodological Overview

3.1. General framework

The general framework presented in Fig. 2 shows the modelling of the relationship between production parameters of the MDF production process and environmental impact indicators using machine learning methods. An experimentally generated dataset was used in the first stage of the study. In this dataset, the variables representing the production process-resin ratio, waste ratio, press temperature, press pressure, and press time-were defined as input parameters. Global warming potential and primary energy demand, representing environmental performance, were considered as model outputs.

Following the preparation of the dataset, the database was organised during the data processing stage and adapted to suit the model development process. At this stage, the dataset was divided into two subsets: training and testing. Eighty per cent of the total data was used for model training, while twenty per cent was set aside as test data to evaluate the model's generalisation performance. This allows the prediction performance of the developed models on previously unseen data to be objectively evaluated. Four different machine learning algorithms were used in the model development phase.

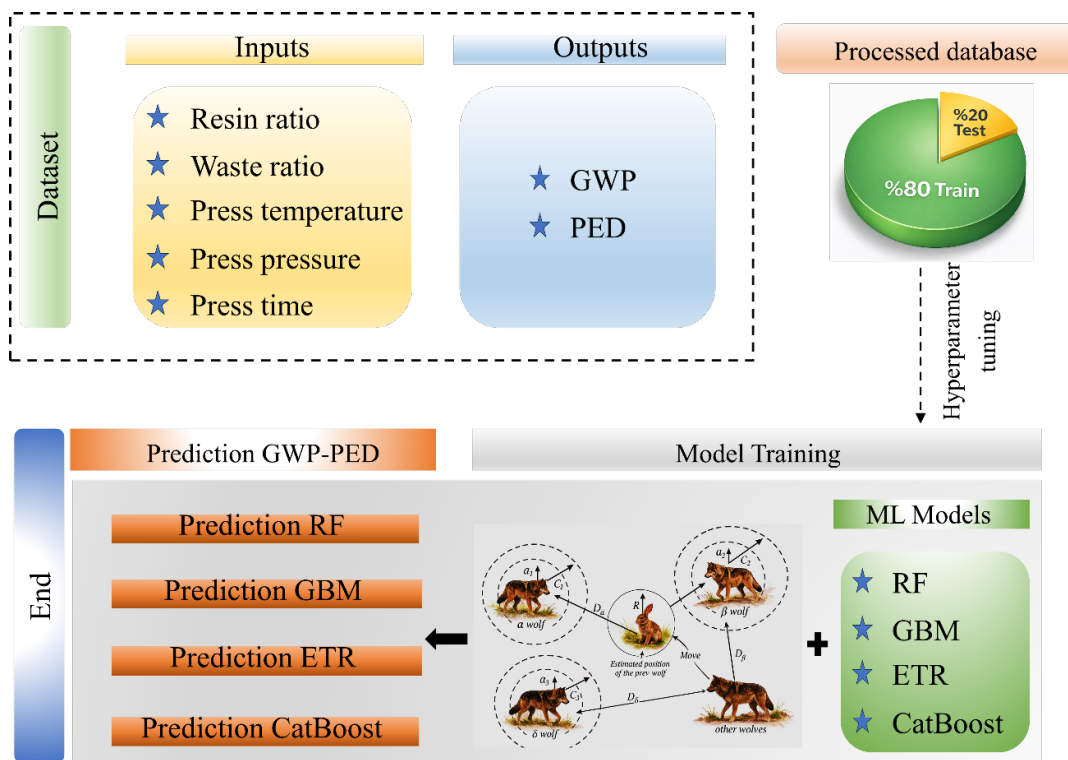


Fig. 2. General framework for study

These are Random Forest, Gradient Boosting Machine, Extra Trees Regressor, and CatBoost methods. Hyperparameter optimisation was applied to improve the performance of these models and determine the most suitable model structures. The Grey Wolf Optimizer algorithm was used in the hyperparameter optimisation process. This algorithm is a meta-heuristic optimisation method that mimics the hunting behaviour of grey wolves and determines the most suitable parameter combination by iteratively updating the model parameters in the search space. Following the optimisation process, machine learning models were trained using the best hyperparameters obtained, and final prediction models were created. In the final stage, these models were used to predict GWP and PED values. Thus, the relationship between production parameters and environmental impacts was revealed based on data, and a modelling framework capable of rapidly predicting the environmental performance of the MDF production process was established.

3.2. Data gathering and description

The dataset used in this study was developed by combining systematically defined MDF production scenarios with life cycle assessment calculations. A total of 60 production scenarios were generated by varying the main controllable process parameters within predefined ranges, including resin ratio, waste fibre ratio, press temperature, press pressure, and press time. For each scenario, GWP and PED outputs were obtained using the LCA model developed in SimaPro.

The functional unit was defined as 1 m³ of MDF to ensure comparability with conventional panel production systems. The system boundary was set as cradle to gate and covered modules A1 to A3, including raw material supply, transport, and manufacturing processes. The MDF production system was structured into process modules consisting of raw material preparation and fibre separation, fibre drying, stepwise heating, resin application and mixing, forming and pre pressing, hot pressing, trimming and sanding, conditioning, and internal logistics. These modules were separately defined in SimaPro to enable traceable modelling of material and energy flows throughout the production line. Electrical and thermal energy inputs were recorded according to energy carrier as kWh and MJ. Resin systems, additives, water use, and process related emissions were assigned to the

relevant production modules. Environmental indicators were calculated in accordance with the LCA framework of ISO 14040, and GWP and PED were selected as the output variables for the machine learning models because they represent the climate impact and primary energy requirement of MDF production. Statistical information regarding these data is provided in Table 1.

The relationship between production parameters and environmental indicators enables the MDF production process to be evaluated in terms of both material usage and energy consumption. The input variables used in this study represent the fundamental operational conditions of the production system, while the output variables demonstrate the effects of these conditions on environmental performance. In particular, the resin ratio, waste fibre ratio, and pressing parameters play a significant role in determining the environmental impacts arising from the production process. Therefore, analysing the relationships between these parameters and environmental impact indicators is critical to understanding the sustainability performance of the production system. The resin ratio refers to the amount of lignin phenol formaldehyde-based binder used in the study within the fibre mixture. Lignin-based resins are considered a more sustainable alternative to traditional phenol formaldehyde systems because they contain a biomass-derived component. However, resin production and use can directly affect the global warming potential of the production system. Changes in resin quantity can also affect the pressing conditions required during panel formation and indirectly alter energy consumption. The waste fibre ratio represents the level at which recycled fibres are incorporated into the raw material mixture during the production process. This parameter plays an important role in reducing primary raw material use and can increase resource efficiency. Although the use of waste fibres has the potential to reduce environmental burdens associated with raw material procurement, differences in fibre quality can create additional energy requirements during production. This situation can have an impact on environmental indicators related to energy consumption. Press temperature, press pressure and press time are the fundamental operational parameters representing the hot pressing stage of the MDF production process.

Table 1. Data description and statistical values

Items	Type	Units	Min	Max	Mean	SD
Resin ratio (lignin)	Input	%	6,04	11,85	9,11	1,70
Waste ratio	Input	%	0,68	29,08	14,32	7,92
Press temperature	Input	°C	166	209,7	186,71	13,33
Press pressure	Input	MPa	2.04	4,92	3,47	0,92
Press time	Input	s	144	316	222,96	54,53
GWP	Output	kg CO ₂ -eq/m ³	435,6	621,5	526,8	48,15
PED	Output	MJ/m ³	5408	7978	6743,3	633

These parameters determine the physical conditions necessary for the compression of fibres and the curing of the binder during panel formation. Changes in pressing conditions can directly affect the amount of thermal and mechanical energy used in the production process. Therefore, these parameters have a significant impact on primary energy demand in particular. Global warming potential and primary energy demand are used as environmental performance indicators in this study. Global warming potential represents the impact of greenhouse gas emissions generated during the production process on climate change, while primary energy demand refers to the total amount of energy used in the production system. Analysing the relationships between input parameters and these environmental indicators enables the identification of operational conditions that increase or decrease environmental impacts in the production system. This relationship also forms the fundamental data structure that allows machine learning models to predict environmental impact indicators based on production parameters.

A Pearson correlation matrix was created to determine the linear relationships between the parameters used in the study. The results of the Pearson correlation analysis reveal linear relationships between the process parameters used in the MDF production process and environmental impact indicators. Examination of the correlation matrix shows that certain production parameters have a more pronounced effect on global warming potential and primary energy demand. According to the results, there is a strong positive relationship between the resin ratio and environmental impact indicators. The correlation coefficient between the resin ratio and global warming potential is calculated as 0.71, while the correlation coefficient with primary energy demand is determined as 0.74. This indicates that the production and use processes of lignin phenol formaldehyde-based binders play a significant role in environmental impacts. It is understood that an increase in the resin ratio could lead to a significant increase, particularly in the total energy requirement and greenhouse gas emissions of the production system. More limited positive relationships are observed between the waste fibre ratio and environmental indicators. The correlation coefficient between the waste ratio and global warming potential is calculated as 0.33, while the correlation coefficient with primary energy demand is 0.39. These values indicate that waste fibre use has a moderate relationship with environmental impacts. Although waste fibre use has the potential to reduce primary raw material consumption, additional processing requirements in the production process can affect energy consumption. When examining pressing parameters, it is seen that pressing time shows a stronger relationship with environmental indicators than other parameters. The correlation coefficient between pressing time and global warming potential is 0.60, while the correlation coefficient with primary energy demand is 0.59. This result indicates that pressing time has a significant effect on the amount of energy

consumed during production. The correlation values between press temperature and press pressure and environmental indicators remain at a lower level. While there is a relationship of approximately 0.31 between press temperature and both environmental indicators, the correlation coefficients with press pressure are calculated as 0.33 and 0.28. In addition to Pearson correlation analysis, multicollinearity among the input parameters was evaluated using the variance inflation factor. The VIF values were calculated together with the model performance metrics for both the training and test datasets. The mean VIF values were 1.048 for the training dataset and 1.788 for the test dataset. Both values were well below the commonly accepted threshold value of 5, indicating that there was no serious multicollinearity among the input variables. Therefore, all process parameters were retained in the model development stage, and variable removal was not required. When examining the relationship between environmental impact indicators, a strong positive correlation is observed between global warming potential and primary energy demand. The correlation coefficient between these two variables is calculated as 0.95. This indicates a strong linear relationship between energy consumption and greenhouse gas emissions in the production process. In other words, an increase in the amount of energy used in the production system directly causes an increase in global warming potential (Fig. 3). Overall, the correlation analysis results show that the resin ratio and press time parameters have more pronounced effects on the environmental performance of the MDF production process. It is understood that these parameters are critical process variables that can affect both energy consumption and emission levels in the production system. Therefore, optimising these parameters offers significant potential for developing improvement strategies aimed at reducing environmental impacts.

3.3. Data preprocessing and hyperparameters tuning

Data quality and methodological consistency are essential for developing reliable machine learning models. In this study, the dataset consisted of 60 production scenarios generated through systematically defined MDF process parameters and corresponding LCA calculations. Since all scenarios were created within predefined operational ranges, all observations were retained in the modelling process. The input variables were resin ratio, waste fibre ratio, press temperature, press pressure, and press time, while the output variables were Global Warming Potential and Primary Energy Demand.

The dataset was divided into training and test subsets using a random splitting procedure. To ensure reproducibility, the random state was fixed at 42. Eighty percent of the dataset was allocated to model training, while the remaining twenty percent was reserved as an independent test set to evaluate predictive performance on unseen data.

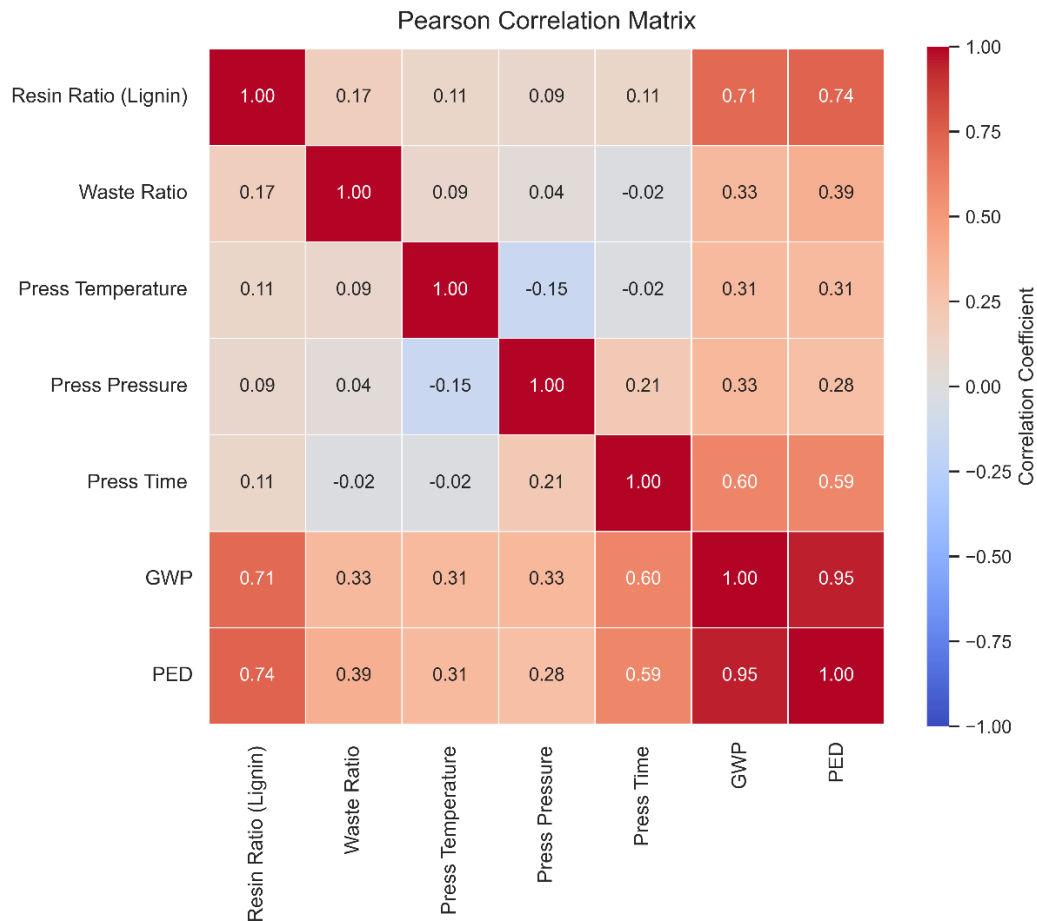


Fig. 3. Pearson correlation matrix

To prevent input variables with larger numerical ranges from dominating the model development process, min max normalization was applied to the input variables by scaling them to the range of 0 to 1. The normalization parameters were determined from the training data and then applied to the test data using the same transformation. This procedure was applied only to the input variables, namely resin ratio, waste fibre ratio, press temperature, press pressure, and press time. The output variables were kept in their original units so that model performance could be evaluated directly in kg CO₂ equivalent per m³ for GWP and MJ per m³ for PED. The training data were used for model fitting and hyperparameter optimisation, whereas the test data were used only for the final performance assessment. This procedure enabled the generalisation performance of the developed models to be evaluated separately from the optimisation process. Since the performance of machine learning models is strongly affected by hyperparameter selection, hyperparameter optimisation was performed during model development. For this purpose, the Grey Wolf Optimizer algorithm was used to search for the most suitable hyperparameter combinations of the Random Forest, Gradient Boosting, Extra Trees, and CatBoost models. The objective function of the GWO based optimisation was defined as the minimisation of the five fold cross validated mean squared error calculated on the training dataset. In the GWO procedure, the population size was set to 50 wolves,

and the maximum number of iterations was set to 100. The stopping criterion was defined as reaching the maximum number of iterations. During the optimisation process, candidate solutions represented different hyperparameter combinations within the predefined search ranges given in Table 2. To improve the reliability and reproducibility of model evaluation during optimisation, a five fold KFold cross validation procedure with shuffling and a fixed random state of 42 was applied on the training dataset. This approach allowed the model performance to be tested across different training and validation partitions.

As a result of the optimisation process, the best hyperparameter combinations were determined separately for each model and each environmental output. Since Global Warming Potential and Primary Energy Demand were modelled as separate target variables, different optimum hyperparameter values were obtained for each output. The hyperparameter search ranges and the best parameter values obtained from the optimisation process are presented in Table 2.

3.4. Model evaluation metrics

Various performance metrics were used to evaluate the prediction performance of the machine learning models developed in this study.

Table 2. ML model hyperparameters

GWO-ML models	Hyper-parameter	Ranges of values	Best values (GWP)	Best values (PED)
GWO-RF	n_estimators	[20 - 1000]	234	225
	max_depth	[3 - 12]	7	12
	min_samples_split	[4 - 16]	4	4
	min_samples_leaf	[2 - 10]	2	2
	max_features	[0.3 - 0.9]	0.625	0.725
GWO-GBM	n_estimators	[20 - 1000]	718	891
	learning_rate	[0.01 - 0.2]	0.044	0.021
	max_depth	[3 - 12]	9	9
	subsample	[0.6 - 1.0]	0.6	0.6
	min_samples_split	[2 - 10]	7	8
GWO-ETR	n_estimators	[20 - 1000]	987	240
	max_depth	[3 - 12]	7	8
	min_samples_split	[4 - 16]	4	4
	min_samples_leaf	[2 - 10]	2	2
	max_features	[0.3 - 0.9]	0.865	0.9
GWO-CatBoost	iterations	[20 - 1000]	1000	787
	depth	[3 - 12]	3	3
	learning_rate	[0.01 - 0.2]	0.077	0.026
	l2_leaf_reg	[3 - 20]	3	3
	Bagging_temperature	[0 - 1]	0	0.523

These metrics enable the assessment of the model's fit between actual values and predicted values from different perspectives. The performance metrics given in Table 3 were used to determine model accuracy, error magnitude, and relative error levels. In addition to these performance metrics, the generalization gap indicators given in Table 3 were used to evaluate the consistency between the training and test performances. The coefficient of determination (R^2) indicates the proportion of variance explained by the model and shows the extent to which the model predictions are consistent with the actual values. An R^2 value close to 1 indicates that the

model can explain the variability in the data set to a large extent. Therefore, the R^2 metric was used to evaluate the explanatory power of the models developed in this study. Root mean square error (RMSE) represents the square root of the average of the squares of the differences between the predicted values and the actual values. This metric measures the absolute error magnitude in model predictions and penalises large errors more heavily. Therefore, the RMSE value is used as an important performance indicator to evaluate the accuracy of model predictions.

Table 3. Performance metrics and generalization gap indicators used in the study

Performance metrics	Formulas
Coefficient of determination (R^2)	$R^2 = 1 - \frac{\sum_{i=1}^n (\text{True}_i - \text{Predicted}_i)^2}{\sum_{i=1}^n (\text{True}_i - \text{True}_{\text{avg}})^2}$
Root mean squared error (RMSE)	$RMSE = \sqrt{\frac{1}{n} \sum_{i=1}^n (\text{True}_i - \text{Predicted}_i)^2}$
Root Mean Squared Relative Error (RMSRE)	$RMSRE = \sqrt{\frac{1}{n} \sum_{i=1}^n \left(\frac{\text{True}_i - \text{Predicted}_i}{\text{True}_i} \right)^2} \times 100$
Relative Root Mean Squared Error (RRMSE)	$RRMSE = \frac{\sqrt{\frac{1}{n} \sum_{i=1}^n (\text{True}_i - \text{Predicted}_i)^2}}{\sum_{i=1}^n \text{True}_i} \times 100$
Mean Absolute Percentage Error (MAPE)	$MAPE = \frac{1}{n} \sum_{i=1}^n \left \frac{\text{True}_i - \text{Predicted}_i}{\text{True}_i} \right $
Coefficient of determination gap (ΔR^2)	$\Delta R^2 = R^2_{\text{training}} - R^2_{\text{test}}$
Root mean squared error gap ($\Delta RMSE$)	$\Delta RMSE = RMSE_{\text{test}} - RMSE_{\text{training}}$

The root mean square relative error (RMSRE) calculates prediction errors by normalising them with actual values. This metric allows for the relative evaluation of error values. Thus, it enables the comparison of model performance across datasets with different scales. In this study, the RMSRE metric was used to evaluate the relative error level of model predictions. The relative root mean square error (RRMSE) is obtained by normalising the RMSE value according to the mean of the observations. This metric allows the model error to be evaluated according to the overall size of the dataset. Thus, model performance can be interpreted independently of the scale of the dataset. The mean absolute percentage error (MAPE) represents the average magnitude of the difference between the predicted values and the actual values as a percentage. This metric facilitates the interpretation of model performance by allowing the model prediction error to be expressed as a percentage. In this study, the MAPE metric was used to evaluate the error level of model predictions as a percentage. The coefficient of determination gap (ΔR^2) and root mean square error gap ($\Delta RMSE$) were also calculated to provide an additional quantitative basis for evaluating model generalization and possible overfitting. When these performance metrics are evaluated together, the machine learning models developed can be comprehensively analysed in terms of both absolute error magnitude and relative error level. This allows for a reliable assessment of the extent to which the models can accurately predict environmental impact indicators such as Global Warming Potential and Primary Energy Demand.

4. Results

4.1. Assessment of machine learning (ML) models

4.1.1. Performance of machine learning (ML) models for global warming potential (GWP)

Figs. 4 and 5 present the Global Warming Potential (GWP) prediction behaviour of the RF and ETR models. Both models provide a generally acceptable agreement between experimental and predicted values, with most predictions remaining close to the ideal line. The RF model shows a relatively wider error spread, particularly in the prediction ratio and residual variation plots, which indicates that its predictions fluctuate more noticeably across the dataset. The ETR model displays a slightly more compact error structure than RF and follows the experimental trend more consistently in several regions of the dataset. Nevertheless, both models show certain deviations in the test region, suggesting that their predictive response is less stable than the boosting based models. Therefore, RF and ETR can be considered reliable baseline ensemble models for GWP estimation, but their performance should be interpreted mainly through the quantitative metrics rather than visual agreement alone.

Figs. 6 and 7 illustrate the GWP prediction results of the GBM and CatBoost models. The GBM model exhibits a balanced prediction pattern, with limited residual dispersion and a close overlap between experimental and predicted trends across both training and test regions. This indicates that GBM captures the variation in GWP values without producing pronounced deviations for most observations.

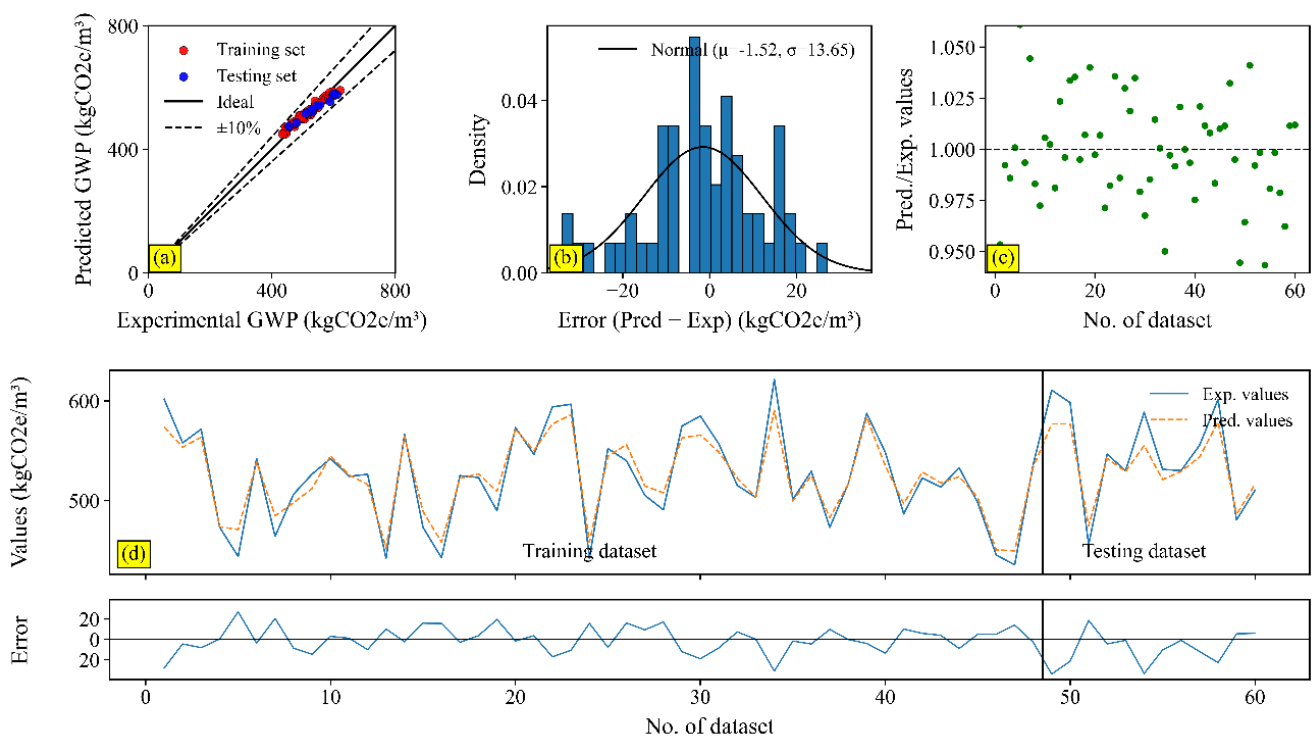


Fig. 4. Performance evaluation of the RF model developed for GWP estimation

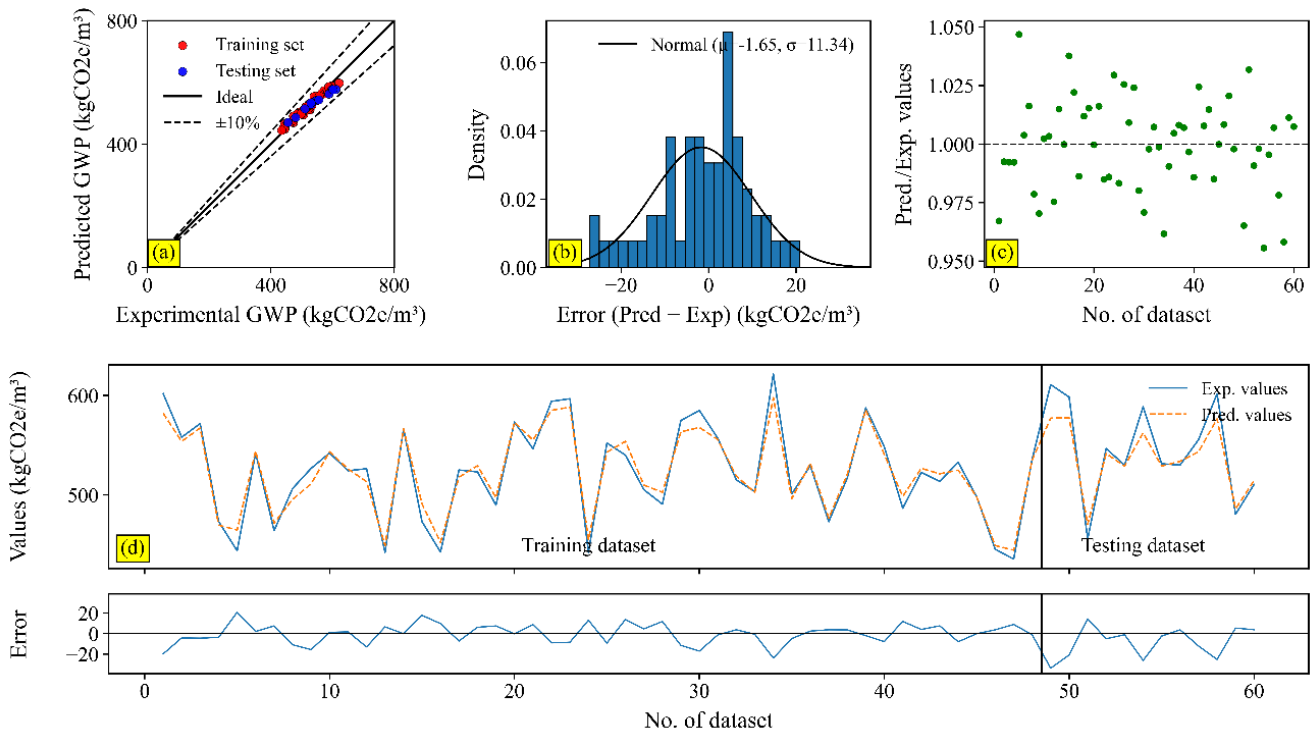


Fig. 5. Performance evaluation of the ETR model developed for GWP estimation

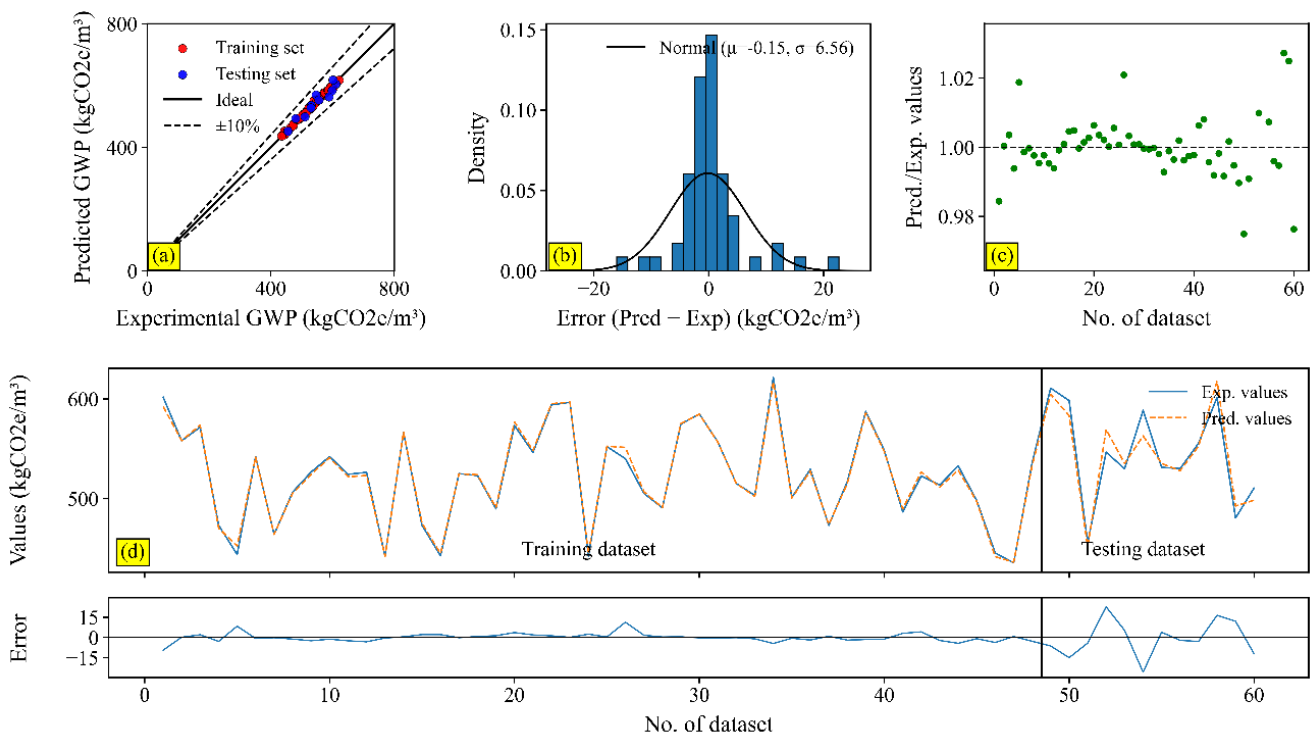


Fig. 6. Performance evaluation of the GBM model developed for GWP estimation

CatBoost, on the other hand, provides an almost exact fit in the training region, but its test predictions show more visible local deviations. This pattern suggests a stronger adaptation to the training data, although the final judgement requires support from independent test metrics. Compared with RF and ETR, the boosting based models provide a more concentrated prediction structure, particularly in the scatter and residual plots. However, the graphical results are used

here only as complementary diagnostic evidence. The comparative performance of the models is evaluated primarily through test set statistics and cross validation results.

When GWP prediction performances are evaluated together, it is seen that all four models generally produce successful results.

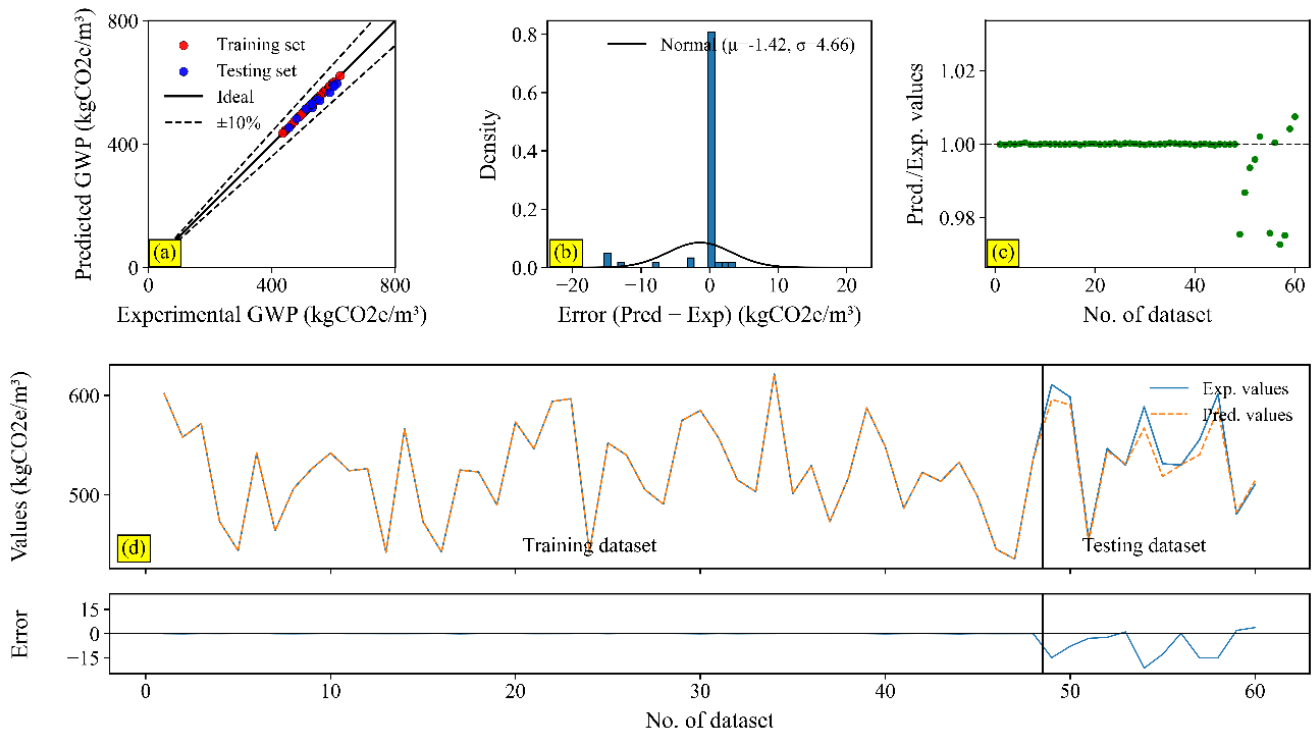


Fig. 7. Performance evaluation of the CatBoost model developed for GWP estimation

In all models, experimental and predicted values are positioned close to the ideal line, and error levels remain limited. However, some relative differences between the models are noteworthy. Although the RF and ETR models produced highly accurate predictions, their error distributions and Pred./Exp. ratios show a wider spread compared to GBM and CatBoost. The GBM model stands out with a more balanced error distribution and a mean error closer to zero, while the CatBoost model is seen to deliver the most stable results, particularly due to the tighter clustering of data points around the 1 reference line and the prediction curve closely following the experimental trend. Overall, while all models demonstrate reliable performance, it can be said that the GBM and, in particular, the CatBoost models offer superior performance in terms of error stability and prediction consistency for GWP estimation.

To evaluate model performance, the metrics R , R^2 , RMSE, RMSRE, RRMSE, and MAPE were examined. Upon reviewing the table, it is observed that all models achieved a high level of accuracy in terms of GWP prediction. Notably, the GWO CatBoost and GWO GBM models stood out in the training dataset with very low error values and high R^2 values. The CatBoost model showed an almost error-free fit in the training data. When evaluating the test data set results, it is seen that all models exhibit strong generalisation performance. However, the highest coefficient of determination ($R^2 = 0.947$) and the lowest error values were obtained in the GWO CatBoost model. The GWO GBM model also performed similarly well. The GWO RF and GWO ETR models produced reliable results but showed slightly lower performance in terms of error metrics

compared to the other two models. Overall, it can be seen that the most successful model for GWP estimation is GWO CatBoost, followed by the GWO GBM model.

For the GWP output, the most notable result was obtained from the GWO CatBoost model, which produced an almost perfect fit in the training dataset. The training R^2 and RMSE values were 1.000 and 0.07, respectively. Since such a high training performance may raise concerns about overfitting, the result was evaluated together with the independent test performance and the generalization gap indicators presented in Table 3. Despite the near perfect training fit, GWO CatBoost maintained a strong predictive performance on the test dataset, with a test R^2 of 0.947 and a test RMSE of 10.81. The ΔR^2 value was 0.053, which was the lowest among the evaluated models. This indicates that the decrease in explanatory performance from training to test data was relatively limited. However, the increase in RMSE from 0.07 to 10.81 shows that the training result should not be interpreted alone as evidence of generalization. GWO GBM also provided a strong alternative for GWP prediction, with a test R^2 of 0.921 and a test RMSE of 13.14. Although its test performance was slightly lower than that of GWO CatBoost, it showed a consistent predictive pattern. GWO RF and GWO ETR produced test R^2 values of 0.851 and 0.873, respectively, indicating acceptable but comparatively lower predictive performance. Taken together, the GWP results suggest that GWO CatBoost provided the highest test accuracy within the investigated experimental domain. Nevertheless, because of its near perfect training fit, the model was interpreted by considering both the test results and the generalization gap

indicators rather than relying only on the training performance (Table 4).

4.1.2. Performance of machine learning (ML) models for primary energy demand (PED)

For PED estimation, the RF and ETR models show comparable prediction behaviour, with both models capturing the general variation pattern of the experimental data. The scatter plots indicate that the predictions are mostly positioned within the $\pm 10\%$ error range, which supports an acceptable level of agreement between measured and predicted PED values. However, the residual and prediction ratio plots reveal that both models exhibit noticeable fluctuations across the dataset. This variation is more evident in the test region, where local deviations between experimental and predicted values become more pronounced. The ETR model appears to provide a slightly narrower error distribution than RF, but the overall prediction behaviour of

the two models remains similar. Accordingly, RF and ETR can be interpreted as models that adequately reflect the main PED response, while their relatively wider residual variation indicates a lower level of prediction consistency compared with the best performing models. This observation is consistent with the quantitative performance results, where both models yielded acceptable but comparatively higher error values (Figs. 8 and 9).

A more compact prediction structure is observed for GBM and CatBoost in Figs. 10 and 11. The GBM model follows the experimental PED profile with relatively small deviations across most observations and maintains a balanced distribution around the reference line in the prediction ratio plot. Its residual pattern also indicates that large errors are limited to a smaller number of observations. CatBoost presents a very close fit in the training region, which is reflected by the dense clustering of prediction ratios around 1 and the narrow residual distribution.

Table 4. Performance metrics for GWP

Models	Dataset	R	R ²	RMSE	RMSRE (%)	RRMSE (%)	MAPE (%)	ΔR^2	$\Delta RMSE$
GWO-RF	Training	0.981	0.932	12.26	2.376	2.347	1.880	0.081	5.80
	Test	0.988	0.851	18.06	3.141	3.314	2.515	0.081	5.80
GWO-ETR	Training	0.985	0.958	9.59	1.846	1.835	1.476	0.085	7.08
	Test	0.992	0.873	16.67	2.859	3.05	2.261	0.085	7.08
GWO-GBM	Training	0.998	0.996	3.13	0.599	0.599	0.406	0.075	10.01
	Test	0.960	0.921	13.14	2.339	2.410	1.933	0.075	10.01
GWO-CatBoost	Training	1	1	0.07	0.013	0.013	0.013	0.053	10.74
	Test	0.990	0.947	10.81	1.870	1.983	1.460	0.053	10.74

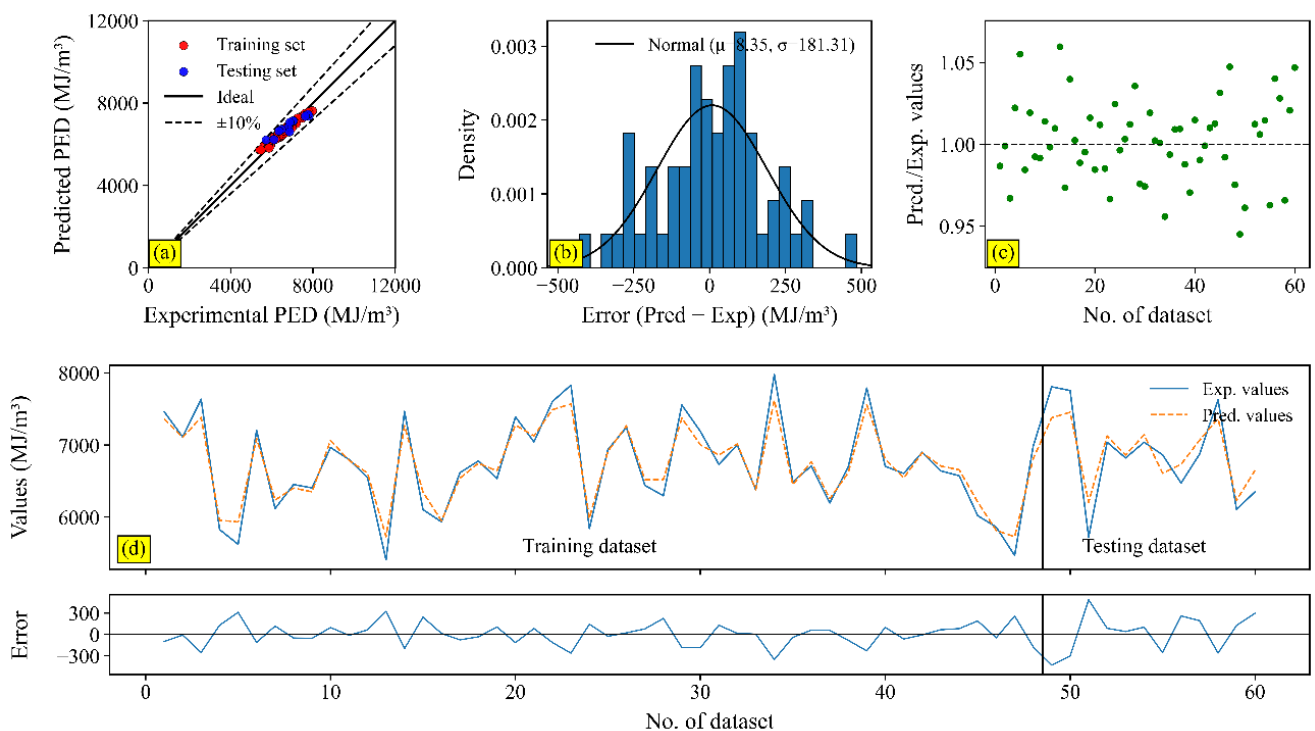


Fig. 8. Performance evaluation of the RF model developed for PED estimation

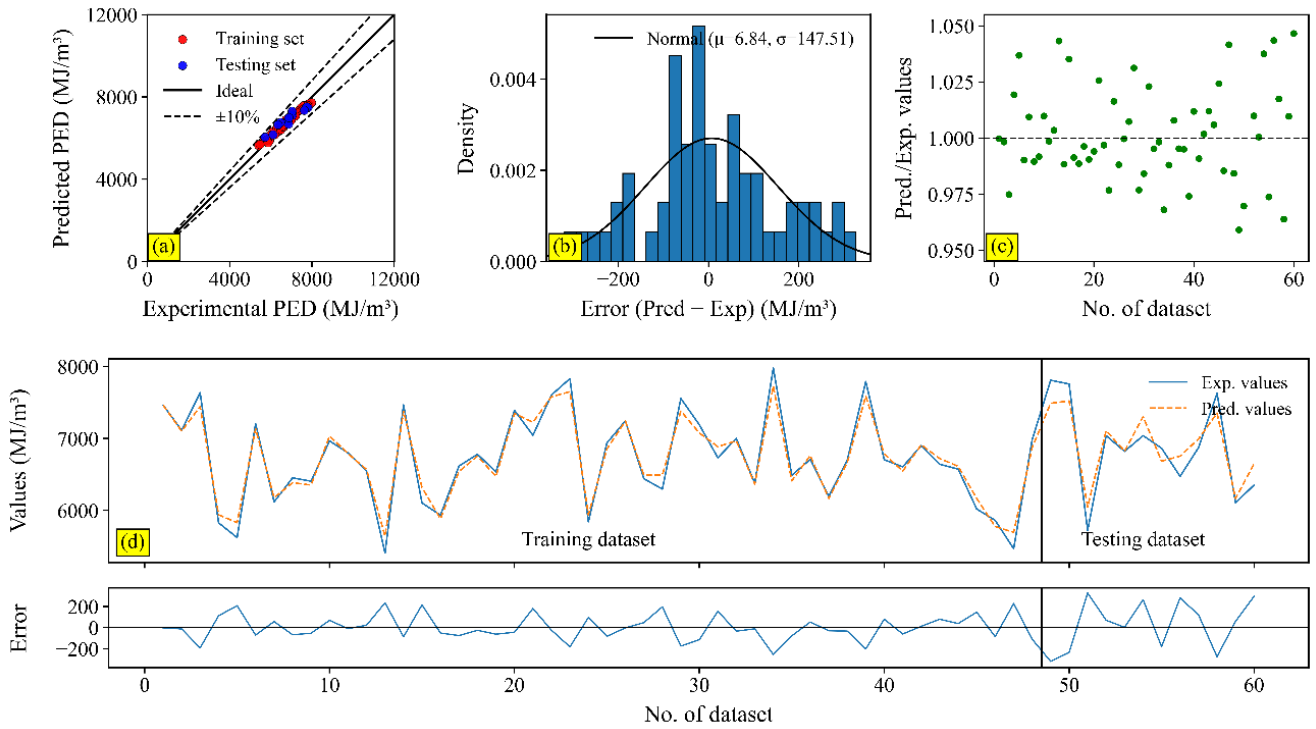


Fig. 9. Performance evaluation of the ETR model developed for PED estimation

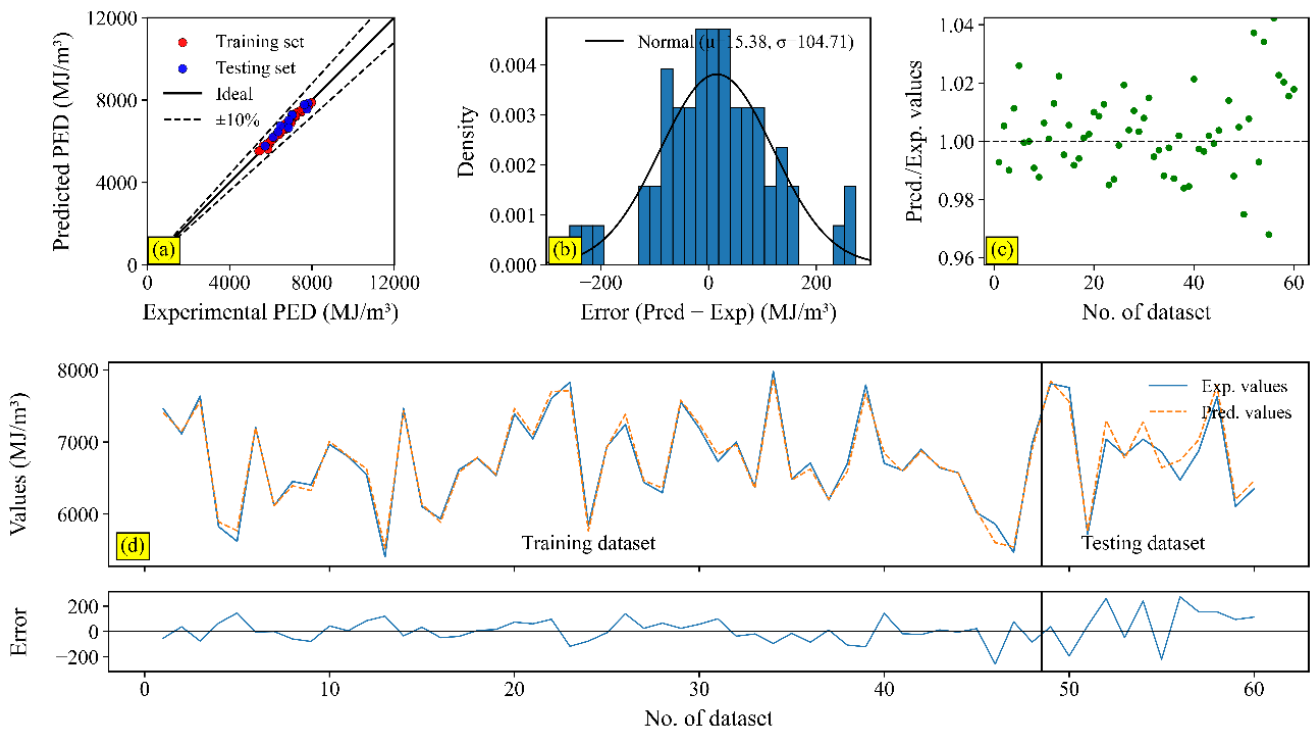


Fig. 10. Performance evaluation of the ETR model developed for PED estimation

In the test region, however, several local deviations are visible, indicating that the model response becomes less uniform for unseen observations. When the two models are considered together, GBM provides a more balanced error structure across the full dataset, whereas CatBoost shows stronger agreement in the training subset but a more variable response in the test subset.

When the PED prediction performances are evaluated together, it is seen that all four models successfully represent

the experimental values and generally achieve a high level of accuracy. In all models, the data points are positioned close to the ideal line, the ratio between the predicted and experimental values is largely clustered around 1, and the error values remain within limited ranges. However, some differences in error distribution and stability are noticeable between the models. While the RF and ETR models produced robust and balanced results, their error spread appears slightly wider compared to GBM and CatBoost.

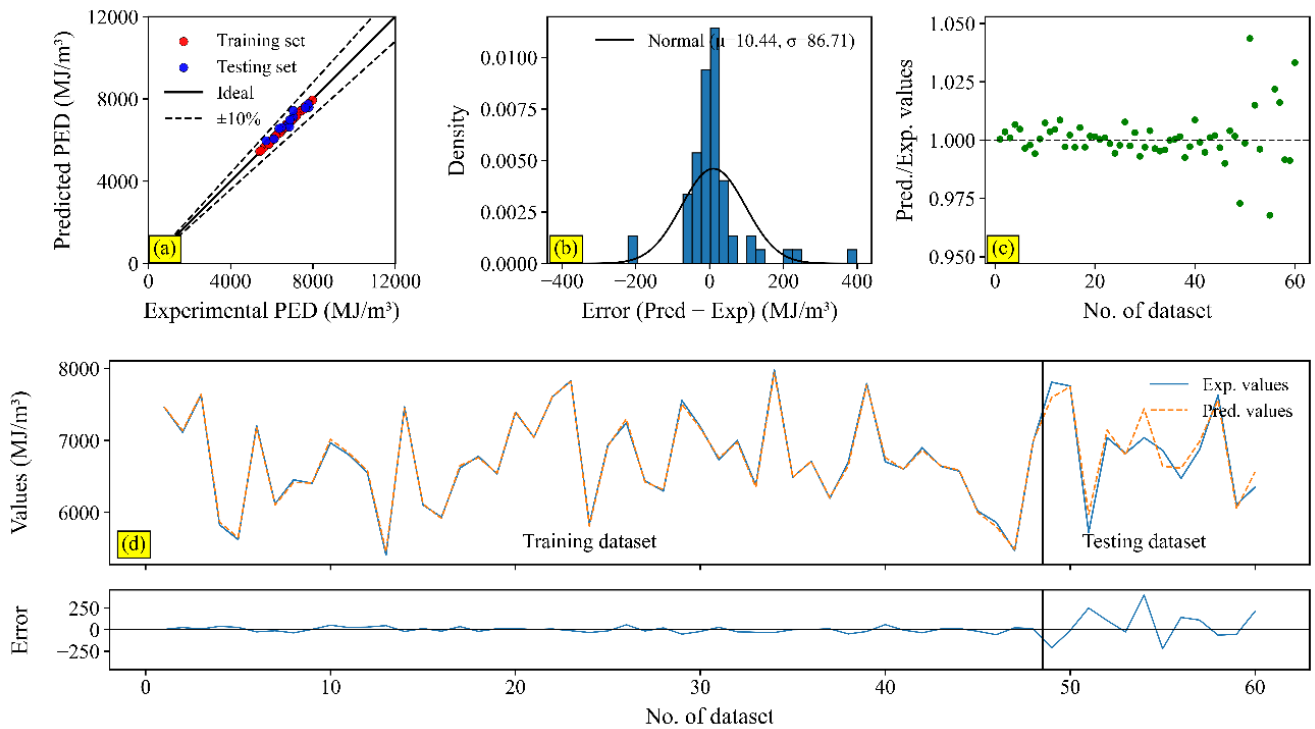


Fig. 11. Performance evaluation of the ETR model developed for PED estimation

The GBM model stands out with a more symmetric error distribution and a more balanced prediction trend throughout the dataset. Although the CatBoost model closely follows the experimental curve, error fluctuations become more pronounced in the latter part of the test dataset compared to other models. Overall, all models demonstrated reliable performance in terms of PED estimation; however, the GBM model showed relatively superior performance in terms of error stability and overall consistency.

To evaluate the PED prediction performance, the accuracy and error levels of the models were analyzed using various performance metrics. Upon examining the table, it is observed that all models achieved high explanatory power values for PED prediction. It is noteworthy that the highest performance in the training dataset was achieved by the GWO CatBoost model, which stood out with low error values and a high R^2 coefficient. When evaluating the test data set results, it is seen that the GWO GBM model has the highest explanatory coefficient ($R^2 = 0.921$) and shows a balanced performance in terms of error metrics. The GWO RF and GWO ETR models also produce reliable results, but their error values are slightly higher than those of other models. Overall, it can be said that the GWO GBM and GWO CatBoost models yield more successful results in PED prediction.

For the PED output, the comparison of the models indicated a different performance pattern from that observed for GWP. In this case, GWO GBM showed the most balanced relationship between training and test results. The model achieved an R^2 value of 0.984 in the training dataset and 0.921 in the test dataset. Its RMSE values were 78.81 for training and 173.92 for testing. The relatively low ΔR^2 value of 0.063 suggests that the predictive structure learned from the training

data was largely preserved in the test dataset. Although GWO CatBoost also showed high test performance, with a test R^2 of 0.911, its training performance was considerably higher. The training R^2 and RMSE values were 0.998 and 28.39, respectively, while the test RMSE increased to 185.16. This larger error increase indicates that the model fitted the training data more strongly than GWO GBM. Therefore, its PED prediction performance was interpreted more cautiously. GWO RF and GWO ETR showed moderate predictive performance for PED, with test R^2 values of 0.811 and 0.863, respectively. These models retained predictive ability on the independent test dataset, but their performance was lower than that of GWO GBM and GWO CatBoost. Overall, the PED results indicate that the model with the highest training performance was not necessarily the most balanced option in terms of generalization. In this output, GWO GBM provided a more stable relationship between training and test performance. Therefore, it was considered to present a more reliable generalization pattern for PED estimation within the studied experimental range (Table 5).

4.2. SHAP and ICE analysis

4.2.1. SHAP and ICE analysis for global warming potential (GWP)

The SHAP method was applied to the CatBoost model, which yielded the best performance in GWP output, to explain the model's decision mechanism and reveal the relative contributions of production parameters to environmental impact. The findings clearly indicate that the most influential variable in GWP estimation is Resin Ratio Lignin (%). This variable is followed by Press Time (s), Press Temperature ($^{\circ}\text{C}$), Waste Ratio (%), and Press Pressure (MPa).

Table 5. Performance metrics for PED

Models	Dataset	R	R ²	RMSE	RMSRE (%)	RRMSE (%)	MAPE (%)	ΔR ²	ΔRMSE
GWO-RF	Training	0.986	0.943	149.29	2.289	2.224	1.789	0.132	120.59
	Test	0.948	0.811	269.88	4.05	3.926	3.491	0.132	120.59
GWO-ETR	Training	0.988	0.965	116.82	1.798	1.740	1.410	0.102	112.61
	Test	0.955	0.863	229.43	3.392	3.337	2.964	0.102	112.61
GWO-GBM	Training	0.992	0.984	78.81	1.226	1.174	0.927	0.063	95.11
	Test	0.968	0.921	173.92	2.517	2.530	2.221	0.063	95.11
GWO-CatBoost	Training	0.999	0.998	28.39	0.434	0.423	0.357	0.087	156.77
	Test	0.959	0.911	185.16	2.757	2.693	2.235	0.087	156.77

The importance graph based on average absolute SHAP values reveals that the resin ratio has a stronger effect than all other variables. This indicates that resin content is the primary determinant of GWP. The distribution graph shows not only the order of importance but also the direction of the effect. Low resin ratios were mostly associated with negative SHAP values. This result indicates that low resin ratios contribute to reducing the GWP value. Conversely, high resin ratios are associated with positive SHAP values. This indicates that as the resin ratio increases, the GWP estimate rises. Similarly, high Press Time values also mostly produced positive SHAP values. This finding suggests that as the pressing time increases, the GWP tends to increase. In the Press

Temperature variable, high temperature values are also generally seen to contribute positively. This result indicates that an increase in temperature has an increasing effect on GWP. The Waste Ratio and Press Pressure variables have a more limited effect. However, high values in these two variables have mostly contributed to increasing GWP. Overall, the results show that GWP is particularly sensitive to resin ratio and energy-intensive pressing conditions. Therefore, the most important areas for intervention in terms of environmental improvement are optimizing the resin ratio, reducing the pressing time, and controlling the pressing temperature (Fig. 12).

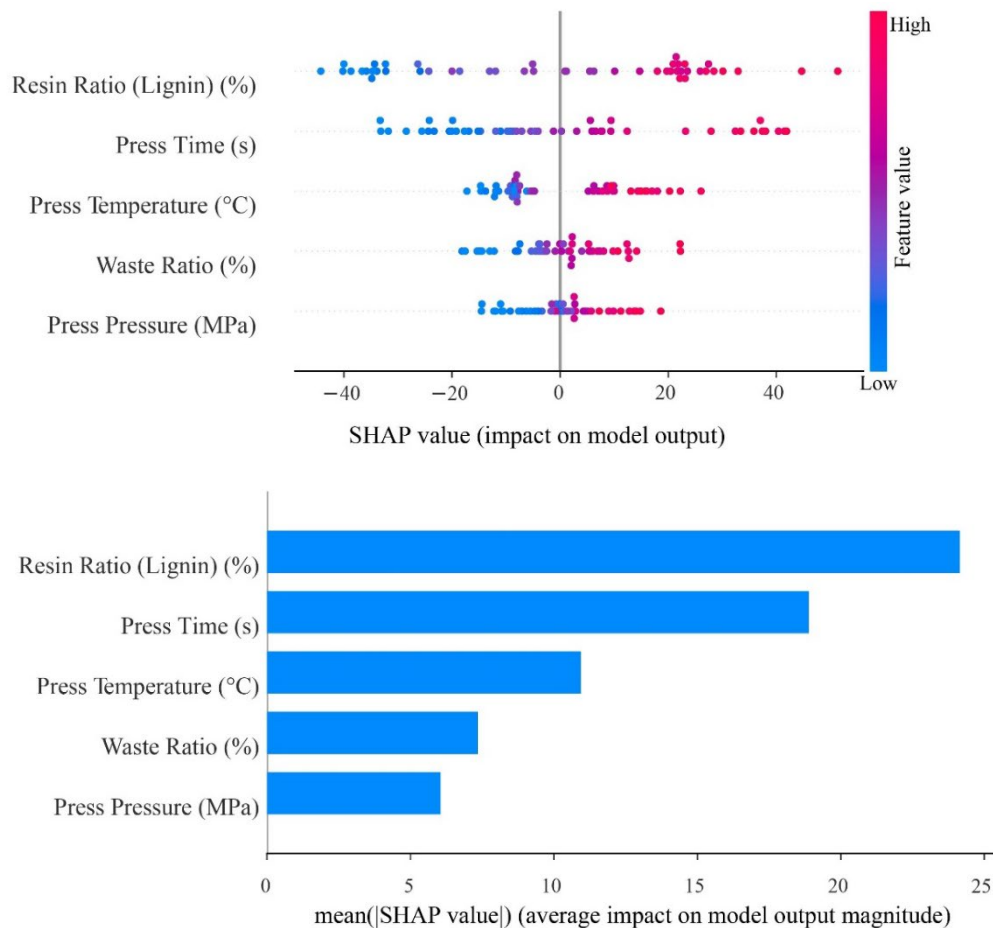


Fig. 12. SHAP charts of the best model for GWP

The ICE graphs obtained for GWP reveal that model predictions show similar trends across all observations and that the environmental impact is particularly sensitive to increases in production parameters. When the graphs are evaluated overall, it is observed that with an increase in the Resin Ratio (Lignin) (%) variable, most GWP predictions rise significantly in most observations. This indicates that the resin ratio has a strong and mostly positive effect on GWP. A similar trend is observed for Press Time (s). As press time increases, a significant portion of the curves move upward, with more pronounced increases in GWP estimates occurring at higher time intervals. The Press Temperature (°C) graph shows that GWP generally increases as temperature rises, but the effect becomes more pronounced in certain ranges. This suggests that temperature has a non-linear but clearly enhancing effect. The lines for Waste Ratio (%) are more

moderate but still mostly upward. This finding indicates that an increase in the waste ratio has an enhancing effect on GWP. For the Press Pressure (MPa) variable, the upward trend is maintained, but the magnitude of the effect is more limited compared to other variables. The fact that the curves are not completely parallel indicates that the variables do not produce the same intensity of effect on different observations and that there are observation-dependent interactions in the model. Overall, these ICE results reveal that GWP is most sensitive to resin content, press time, and press temperature, while waste ratio and press pressure contribute in a secondary but still enhancing manner. Therefore, optimization of resin usage, reduction of pressing time, and careful control of temperature conditions should be prioritized as intervention areas in improvement strategies aimed at reducing GWP (Fig. 13).

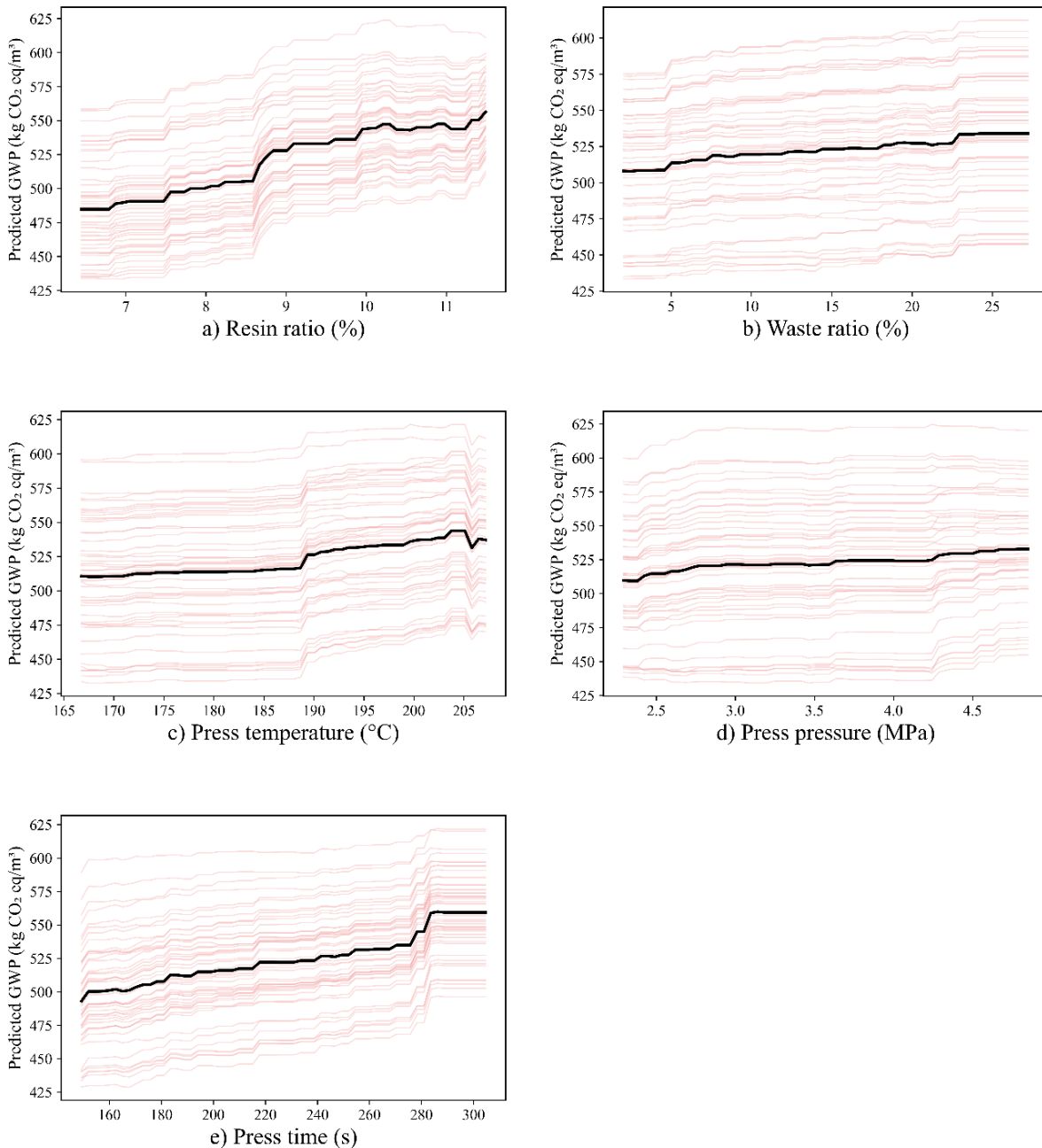


Fig. 13. ICE graphs of the best model for GWP

4.2.2. SHAP and ICE analysis for primary energy demand (PED)

The evaluation of the PED output using the SHAP method on the GBM model that delivers the best performance was conducted to explain the model's decision structure and reveal the effects of production parameters on primary energy demand. The results obtained clearly show that the most effective variable in PED estimation is Resin Ratio Lignin (%). This variable is followed by Press Time (s). Press Temperature (°C) and Waste Ratio (%) show a similar level of impact, while Press Pressure (MPa) stands out as the variable with the lowest contribution. The importance graph based on average absolute SHAP values reveals that the resin ratio and press time have a significantly higher explanatory power than the other variables. The scatter plot clearly shows the direction of this effect. Low Resin Ratio Lignin values were mostly associated with negative SHAP values. High values produced strong positive SHAP contributions. This indicates that as the resin ratio increases, the PED prediction increases significantly. Similarly, high Press Time values are mostly associated with positive SHAP values, suggesting that longer pressing times have an increasing effect on PED. In the Press Temperature variable, high temperature values generally contribute positively. This finding indicates that

temperature increases have an upward effect on energy demand. For Waste Ratio, low values are mostly associated with negative SHAP contributions, while high values are associated with positive contributions. This result indicates that an increase in the waste ratio has a negative effect on PED. Although the Press Pressure variable has a more limited effect compared to the others, the fact that high pressure values mostly produce positive SHAP contributions suggests that this variable also plays a role in increasing energy demand. Overall, the results show that PED is particularly sensitive to resin ratio and pressing time, while temperature and waste ratio also contribute in a secondary but meaningful way. Therefore, the primary strategies for improving energy performance should be optimizing the resin ratio, reducing the pressing time, carefully controlling the press temperature, and lowering the waste ratio (Fig. 14).

ICE graphs created based on the GBM model for PED show that primary energy demand generally responds with an upward trend to all production variables and that this response includes stronger threshold behaviors in some variables. Specifically, in the Resin Ratio (Lignin) (%) graph, the upward shift of the curves with more pronounced jumps after certain intervals reveals that an increase in the resin ratio has a strong and non-linear effect on PED.

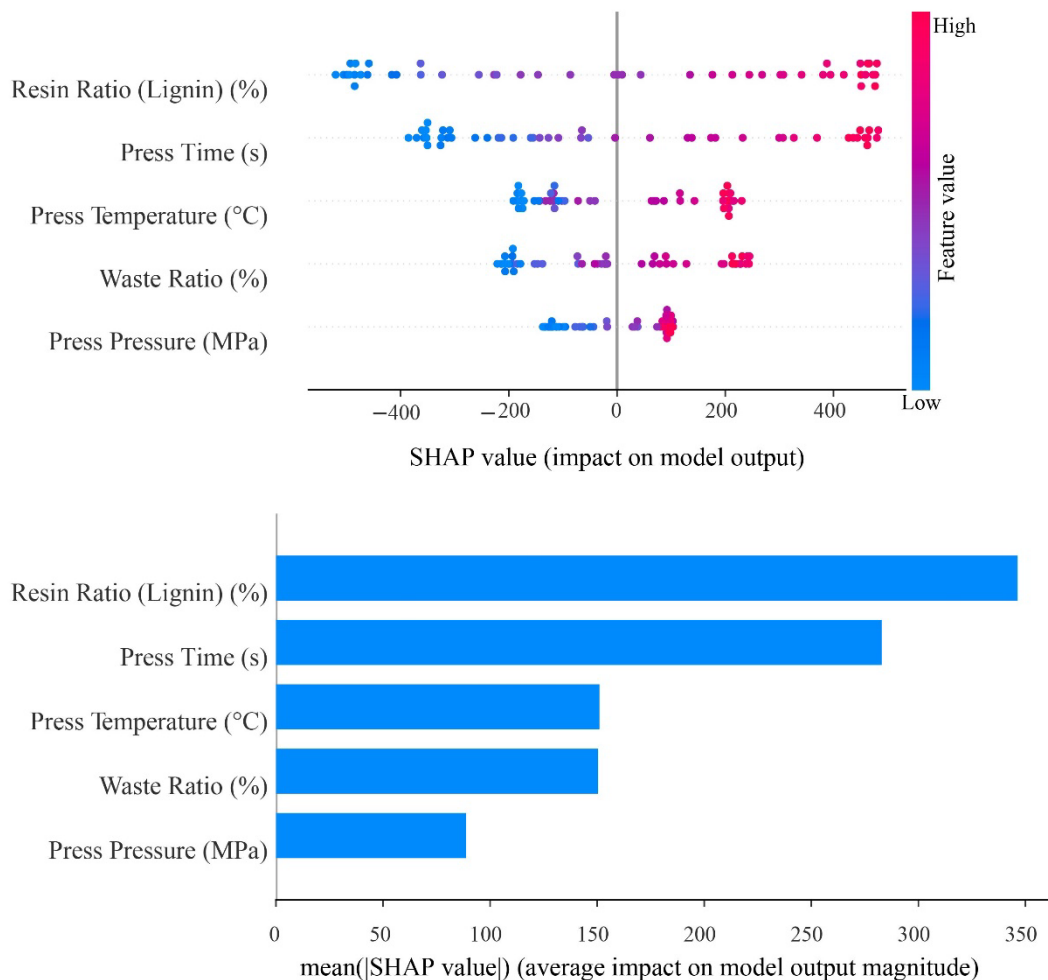


Fig. 14. SHAP charts of the best model for PED

Similarly, along the Press Time (s) variable, most of the curves rise steadily, indicating that longer press times systematically increase energy demand. The pattern obtained for Press Temperature ($^{\circ}\text{C}$) suggests that the increase in temperature contributes more significantly, especially in the medium and high ranges. The sudden directional changes observed in some sections indicate that the model's response to temperature is not constant but more sensitive within specific process ranges. The Waste Ratio (%) graph also reveals that PED is sensitive to increases in the waste ratio. In most curves, a gradual increase is observed as waste levels rise from low to high, supporting the role of material losses in increasing energy demand. In the Press Pressure (MPa) variable, while the upward trend is maintained, the steeper slopes indicate that the effect of this parameter on PED is

weaker than other variables but still positive. Looking at the curves as a whole, the fact that the lines run largely parallel indicates that the model establishes a similar general response structure across observations, while the divergences in some intervals indicate interactions between variables and observation-specific heterogeneity. In conclusion, these graphs reveal that PED is primarily driven by resin content, press time, and press temperature, with the waste ratio acting as an additional driving force and press pressure playing a more secondary role. Within this framework, reducing resin usage, shortening processing time, optimizing temperature conditions, and limiting waste generation can be considered priority areas for improvement in production strategies aimed at enhancing energy performance (Fig. 15).

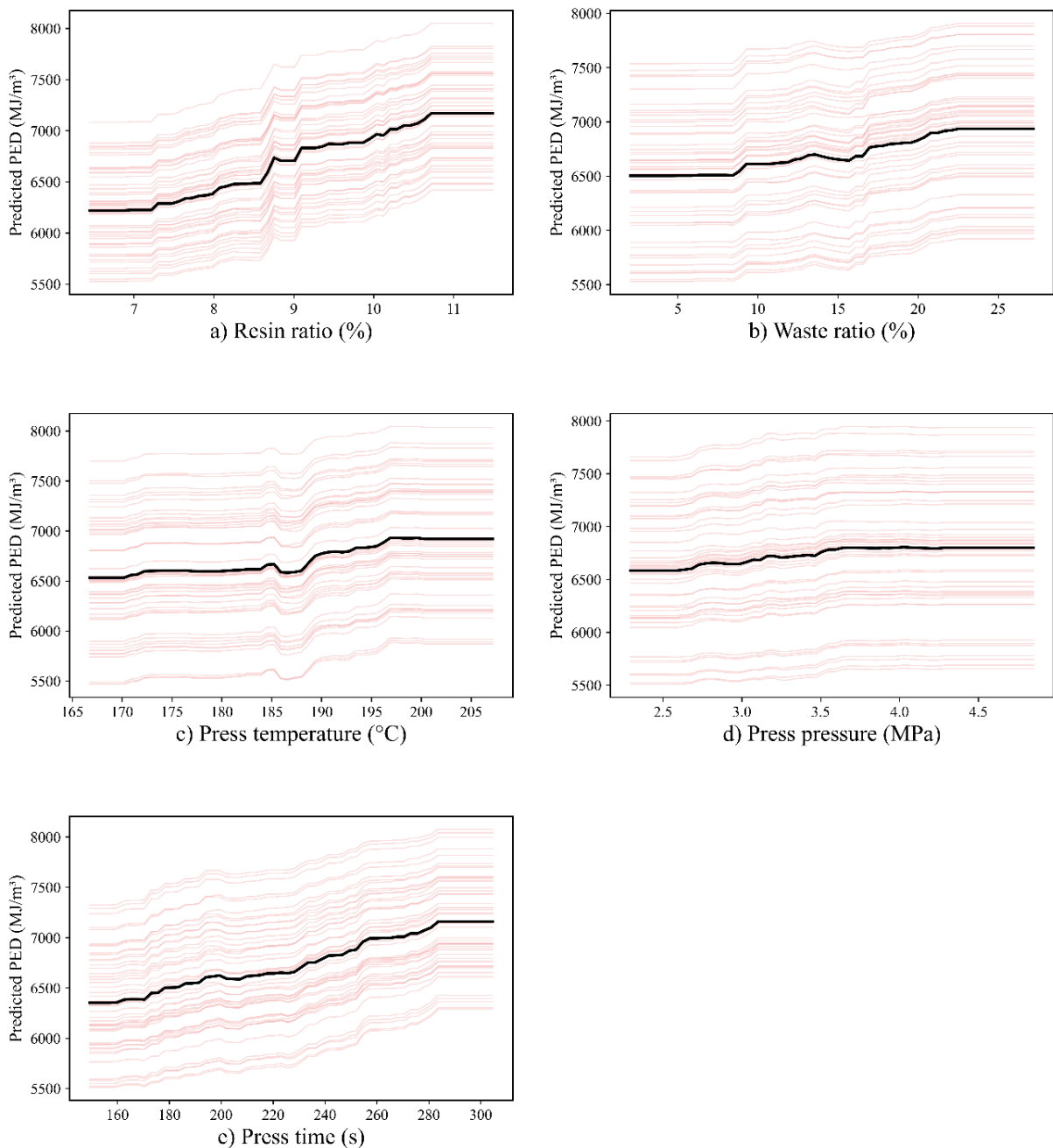


Fig. 15. ICE graphs of the best model for PED

5. Discussion

In this study, GBM, ETR, CatBoost, and RF models optimized with GWO were used to predict GWP and PED outputs from controllable process variables in MDF production. The results showed that the best performance for GWP was achieved with the CatBoost model, while the best performance for PED was achieved with the GBM model. When SHAP and ICE analyses were evaluated together, it was observed that the strongest effect on both outputs was related to the resin ratio, followed by press time and press temperature. Although the waste ratio and press pressure were also effective, their contribution was more limited. These findings indicate that the environmental load in MDF production is strongly dependent not only on material usage but also on energy intensive pressing conditions. This general trend is largely consistent with the current LCA literature. In a cradle to gate LCA study conducted for melamine-coated MDF production in Turkey, it was shown that the fiber preparation stage is the main critical point and that UF resin and electricity consumption significantly increase environmental impacts [5]. A study comparing MDF and particleboard in China also reported that MDF has a higher environmental impact, with resin consumption and electricity usage among the main reasons for this [6]. In the current study, the resin ratio emerged as the dominant variable on both GWP and PED, while press time and temperature also ranked high, which is consistent with these results. However, what distinguishes this study is that it not only identifies critical points in production at the process level but also makes them predictable and rankable directly through production variables. The findings regarding the waste ratio are also consistent with the literature. It has been reported that redirecting wood waste to panel production can provide environmental benefits, but this depends on appropriate quality and process conditions [32]. According to this study, the increase in environmental burden with rising waste rates in the current model reflects inefficiency in the waste generation phase, while the literature indicates that waste can be transformed into a circular advantage when managed properly.

The dominance of resin content as a key variable is supported not only by LCA studies but also by publications focusing on machine learning and process optimization in wood based materials. A recent study compiling machine learning applications in wood materials has demonstrated that ML has become a powerful tool, particularly in the areas of property prediction, defect detection, and optimized design [33]. The compilation combining LCA with machine learning also emphasizes that ML methods can be effectively used in environmental impact prediction and optimization scenarios [34]. Within this framework, the current study contributes to the literature by utilizing machine learning in wood composite production not only for quality or mechanical performance

but also for directly estimating environmental indicators such as GWP and PED. Furthermore, making model decisions explainable using SHAP and ICE enhances the methods applicability for industrial decision support.

The findings indicate that environmental improvement in MDF production should not be interpreted through a single process parameter but through a complementary process management approach. Reducing resin content, optimizing press time and temperature, limiting unnecessary pressure loads, and reducing waste at source while directing it to appropriate recovery scenarios should be considered collectively. However, the applicability of the developed models is limited to the production scenarios, input parameter ranges, and LCA assumptions considered in this study. Therefore, the models should not be extrapolated beyond the investigated ranges of resin ratio, waste fibre ratio, press temperature, press pressure, and press time. Since GWP and PED values were calculated based on the defined cradle to gate LCA framework, the results are also dependent on the selected system boundary, inventory structure, and process assumptions. In addition, the models were developed using a limited dataset consisting of 60 scenarios. Therefore, further validation with larger datasets and industrial scale production data is required before the models can be generalized to different MDF production systems. Within these boundaries, the proposed framework should be interpreted as a process specific decision support tool that complements conventional LCA reporting through data driven and explainable machine learning.

6. Conclusions

In this study, machine learning models capable of quickly, reliably, and transparently estimating the GWP and PED indicators—directly controllable process variables in MDF production—were developed. RF, ETR, GBM, and CatBoost algorithms optimized with GWO were compared. The performance results obtained showed that CatBoost was the best model for GWP prediction. This model produced $R^2 = 0.9467$, RMSE = 10.81, MAE = 8.31, and MAPE = 1.46% values in the test data. GBM achieved the best performance in PED prediction. The GBM model achieved $R^2 = 0.9214$, RMSE = 173.92, MAE = 153.23, and MAPE = 2.22% on the test data. These results show that the developed models can predict both environmental indicators with a high level of accuracy.

Interpretability analyses have demonstrated that the results are not only accurate but also explainable. According to SHAP and ICE analyses, the resin ratio had the strongest impact on both GWP and PED. This variable was followed by press time and press temperature. Waste ratio and press pressure also contributed to a lesser extent but still significantly. In particular, the fact that an increase in resin ratio has a significant enhancing effect on both outputs indicates that a significant portion of the environmental

burden in MDF production is related to binder usage and energy-intensive process conditions. The fact that increases in press time and temperature also raise GWP and PED values clearly demonstrates the critical role of process parameters in environmental performance.

The main contribution of this study is that it presents a data-driven decision support framework that can predict and interpret the results of classical life cycle assessments based on production parameters, rather than simply reporting these results. This reduces the computational load required for

scenario analysis, while also making priority areas for environmental improvement numerically visible. Consequently, optimizing the resin ratio, carefully managing the pressing time and temperature, reducing waste generation, and holistically controlling the process window emerge as key strategies for reducing both the climate impact and energy demand in MDF production. In this regard, the study demonstrates that environmental eco-efficiency in wood composite production can be improved through explainable machine learning-supported process management.

Declarations

Conflict of Interests

The authors declared no potential conflicts of interest with respect to the research, authorship, and/or publication of this article.

Funding

This research received no external funding.

Author Contributions

C. Yetis: Conceptualization, Methodology, Software, Validation, Formal analysis, Investigation, Resources, Data curation, Writing-Original draft, Visualization M. Tuna Kayılı: Writing - Review & Editing, Supervision, Project administration, Funding acquisition.

Acknowledgments

Not applicable.

Data Availability Statement

The data presented in this study are available on request from the corresponding author.

Ethics Committee Permission

Not applicable.

Use of Generative AI and AI-assisted Technologies

The author confirms the author did not use any AI tools in the preparation of this study.

References

- [1] Jin C, Zhu S, Feng H (2025) Life cycle assessment of engineered wood products in the building sector: a review. *Buildings* 15:4193. <https://doi.org/10.3390/buildings15224193>.
- [2] Dasiewicz J, Wronka A, Ježo A, Kowaluk G (2024) Thermally active medium-density fiberboard (MDF) with the addition of phase change materials for furniture and interior design. *Materials* 17:4001. <https://doi.org/10.3390/ma17164001>.
- [3] Gul W, Ahmad N, Mohammad S, Salah B, Sajid Ullah S, Khurram M, Khan R (2023) Impact of moisture content, closing speed, and pressurizing speed on the performance of medium density fiberboard (MDF). *Frontiers in Materials* 10:1195789. <https://doi.org/10.3389/fmats.2023.1195789>.
- [4] Lee S-H, Batjargal B-U, Kang M, Kwak HW, Han H, Lee Y, Kim J, Lee K, Yeo H (2025) A study on the moisture content and energy efficiency change in wood fiber drying over time using a fluidized bed dryer. *Journal of Korean Wood Science and Technology* 53:693–702. <https://doi.org/10.5658/wood.2025.53.6.693>.
- [5] Yılmaz E (2024) Environmental impact assessment of melamine coated medium density fiberboard (MDF-LAM) production and cumulative energy demand: a case study in Türkiye. *Case Studies in Construction Materials* 20. <https://doi.org/10.1016/j.csem.2023.e02733>.
- [6] Lao W-L, Chang L (2023) Comparative life cycle assessment of medium density fiberboard and particleboard: a case study in China. *Industrial Crops and Products* 205:117443. <https://doi.org/10.1016/j.indcrop.2023.117443>.
- [7] Costa D, Serra J, Quinteiro P, Dias AC (2024) Life cycle assessment of wood-based panels: a review. *Journal of Cleaner Production* 444:140955. <https://doi.org/10.1016/j.jclepro.2024.140955>.
- [8] Heroux G, Puettmann M (2023) Cradle-to-grave life cycle assessment of North American medium density fiberboard.
- [9] Pierzchalski M (2026) Wood and wood-based products in construction: carbon sequestration, emissions and end-of-life scenarios. <https://doi.org/10.53502/wood-209238>.
- [10] BAU (2024) Product category rules for building related products. Part B: Requirements on the EPD for wood and wood-based products.
- [11] BRE (2023) BRE Global Product Category Rules (PCR) for Type III Environmental Product Declarations of Construction Products to EN 15804+A2.
- [12] Calvez I, Garcia R, Koubaa A, Landry V, Cloutier A (2024) Recent advances in bio-based adhesives and formaldehyde-free technologies for wood-based panel manufacturing. *Current Forestry Reports* 10:386–400. <https://doi.org/10.1007/s40725-024-00227-3>.
- [13] Paez J, Fatehi P (2025) Incorporation of lignin into adhesives: a review. *Green Chemistry* 27:12499–12537. <https://doi.org/10.1039/D5GC02998H>.
- [14] Siahkamari M, Emmanuel S, Hodge DB, Nejad M (2022) Lignin-glyoxal: a fully biobased formaldehyde-free wood

- adhesive for interior engineered wood products. *ACS Sustainable Chemistry & Engineering* 10:3430–3441. <https://doi.org/10.1021/acssuschemeng.1c06843>.
- [15] Ahire JP, Mousavi-Avval SH, Rajendran N, Bergman R, Runge T, Jiang C, Hu J (2024) Techno-economic and life cycle analyses of bio-adhesives production from isolated soy protein and kraft lignin. *Journal of Cleaner Production* 447:141474. <https://doi.org/10.1016/j.jclepro.2024.141474>.
- [16] Forssell S, Bangalore Ashok RP, Henn KA, Tirronen E, Toivonen J, Osterberg M, Oinas P (2025) Techno-economic assessment of the industrial-scale production of epoxidized kraft lignin for adhesives or coatings. *ACS Sustainable Chemistry & Engineering* 13:3200–3208. <https://doi.org/10.1021/acssuschemeng.4c09146>.
- [17] Yang M, Rosentrater KA (2020) Life cycle assessment of urea-formaldehyde adhesive and phenol-formaldehyde adhesives. *Environmental Processes* 7:553–561. <https://doi.org/10.1007/s40710-020-00432-9>.
- [18] Arias A, González-García S, González-Rodríguez S, Feijoo G, Moreira MT (2020) Cradle-to-gate life cycle assessment of bio-adhesives for the wood panel industry: a comparison with petrochemical alternatives. *Science of the Total Environment* 738:140357. <https://doi.org/10.1016/j.scitotenv.2020.140357>.
- [19] Wang H (2025) Integrating machine learning into life cycle assessment: review and future outlook. *PLOS Climate* 4. <https://doi.org/10.1371/journal.pclm.0000732>.
- [20] Romeiko XX, Zhang X, Pang Y, Gao F, Xu M, Lin S, Babbitt C (2024) A review of machine learning applications in life cycle assessment studies. *Science of the Total Environment* 912:168969. <https://doi.org/10.1016/j.scitotenv.2023.168969>.
- [21] Neupane B, Belkadi F, Formentini M, Rozière E, Hilloulin B, Abdolmaleki SF, Mensah M (2025) Machine learning algorithms for supporting life cycle assessment studies: an analytical review. *Sustainable Production and Consumption* 56:37–53. <https://doi.org/10.1016/j.spc.2025.03.015>.
- [22] Blanco CF, Pauliks N, Donati F, Engberg N, Weber J (2024) Machine learning to support prospective life cycle assessment of emerging chemical technologies. *Current Opinion in Green and Sustainable Chemistry* 50:100979. <https://doi.org/10.1016/j.cogsc.2024.100979>.
- [23] Kumar D, Maurya KK, Mandal SK, Mir BA, Nurdiawati A, Al-Ghamdi SG (2025) Life cycle assessment in the early design phase of buildings: strategies, tools, and future directions. *Buildings* 15:1612. <https://doi.org/10.3390/buildings15101612>.
- [24] Yenkie KM, Aboagye EA, Lehr AL, Pazik J, Longo J, Hesketh RP (2024) Machine learning enabled life cycle assessment for early-stage sustainable process design. *Computer Aided Chemical Engineering* 53:2881–2886. <https://doi.org/10.1016/B978-0-443-28824-1.50481-6>.
- [25] de Paula Salgado I, Conrad F, Signorini C, Günther E, Ihlenfeldt S, Mechtcherine V (2025) Integrating life cycle assessment (LCA) and machine learning for sustainable designs: a case study on protective layers made of mineral-bonded fiber-reinforced composites. *International Journal of Life Cycle Assessment* 30:1–20. <https://doi.org/10.1007/s11367-025-02454-7>.
- [26] Saves P, Palar PS, Robani MD, Verstaavel N, Garouani M, Aligon J, Gaudou B, Shimoyama K, Morlier J (2025) Surrogate modeling and explainable artificial intelligence for complex systems: a workflow for automated simulation exploration. *arXiv preprint arXiv:2510.16742*. <https://doi.org/10.48550/arXiv.2510.16742>.
- [27] Breiman L (2001) Random forests. *Machine Learning* 45:5–32. <https://doi.org/10.1023/A:1010933404324>.
- [28] Friedman JH (2001) Greedy function approximation: a gradient boosting machine. *Annals of Statistics* 29:1189–1232. <https://doi.org/10.1214/aos/1013203451>.
- [29] Geurts P, Ernst D, Wehenkel L (2006) Extremely randomized trees. *Machine Learning* 63:3–42. <https://doi.org/10.1007/s10994-006-6226-1>.
- [30] Prokhorenkova L, Gusev G, Vorobev A, Dorogush AV, Gulin A (2018) CatBoost: unbiased boosting with categorical features. *Advances in Neural Information Processing Systems* 31.
- [31] Mirjalili S, Mirjalili SM, Lewis A (2014) Grey wolf optimizer. *Advances in Engineering Software* 69:46–61. <https://doi.org/10.1016/j.advengsoft.2013.12.007>.
- [32] Amarasinghe IT, Qian Y, Gunawardena T, Mendis P, Belleville B (2024) Composite panels from wood waste: a detailed review of processes, standards, and applications. *Journal of Composites Science* 8:417. <https://doi.org/10.3390/jcs8100417>.
- [33] Feng Y, Mekhilef S, Hui D, Chow CL, Lau D (2024) Machine learning-assisted wood materials: applications and future prospects. *Extreme Mechanics Letters* 71:102209. <https://doi.org/10.1016/j.eml.2024.102209>.
- [34] Ghoroghi A, Rezguy Y, Petri I, Beach T (2022) Advances in application of machine learning to life cycle assessment: a literature review. *International Journal of Life Cycle Assessment* 27:433–456. <https://doi.org/10.1007/s11367-022-02030-3>.